Published in final edited form as:
J Med Chem. 2016 December 22; 59(24): 10994–11005. doi:10.1021/acs.jmedchem.6b01109.

Truncated Latrunculins as Actin Inhibitors *Targeting Plasmodium falciparum* Motility and Host-Cell Invasion

Swapna Johnson[†,‡], **Raphaël Rahmani**[‡], **Damien R. Drew**[§], **Melanie J. Williams**[¶], **Mark Wilkinson**[#], **Yan Hong Tan**[¶,#], **Johnny X. Huang**[¥], **Christopher J. Tonkin**[¶], **James G. Beeson**[§], **Jake Baum**[¶,#,*], **Brian J. Smith**[†,*], **Jonathan B. Baell**[‡,*]

[†]La Trobe Institute for Molecular Science, La Trobe University, Melbourne Victoria 3086, Australia

[‡]Monash Institute of Pharmaceutical Sciences, Monash University, Parkville Victoria 3052, Australia

[§]Burnet Institute, 85 Commercial Rd, Melbourne Victoria 3004, Australia. Central Clinical School and Department of Microbiology, Monash University, Melbourne Victoria 3004, Australia

[¶]Walter and Eliza Hall Institute, 1G Royal Parade, Parkville Victoria 3052, Australia

[#]Department of Life Sciences, Imperial College, London, South Kensington, SW7 2AZ, UK

[¥]Institute for Molecular Bioscience, The University of Queensland, St Lucia Queensland 4072, Australia

Abstract

Polymerization of the cytosolic protein actin is critical to cell movement and host-cell invasion by the malaria parasite, *Plasmodium falciparum.* Any disruption to actin polymerization dynamics will render the parasite incapable of invading a host cell and thereby unable to cause infection. Here, we explore the potential of using truncated latrunculins as potential chemotherapeutics for the treatment of malaria. Exploration of the binding interactions of the natural actin inhibitor latrunculins, with actin revealed how a truncated core of the inhibitor could retain its key interaction features with actin. This truncated core was synthesised and subjected to preliminary structure-activity relationship studies to generate a focused set of analogues. Biochemical analyses of these analogues demonstrate their 6-fold increased activity compared with latrunculin B against *Plasmodium falciparum* and a 16-fold improved selectivity *ex vivo*. These data establish the latrunculin core as a potential focus for future structure-based drug design of chemotherapeutics against malaria.

[*]Correspondence to: Jake Baum, Jake.baum@imperial,ac,uk; phone, +44 (0)20 759 45420, Brian J. Smith, brian.smith@latrobe.edu.au; phone, +61 3 9479 3245, Jonathan B. Baell, jonathan.baell@monash.edu; phone, +61 3 9903 9044.

Author Contributions

JB, BJS and JBB conceived of the study and designed most of the experiments. SJ performed the chemical synthesis with guidance and assistance from RR. SJ wrote and all authors edited the manuscript. DRD and JGB performed the *P.falciparum* growth inhibition assay, MJW and CJT performed the *T.gondii* invasion inhibition assay, MW, YHT and JB performed the pyrene fluorescence assay and JXH performed the cytotoxicity assay.

Competing financial interests

The authors have no competing financial interests to disclose.

Europe PMC Funders Author Manuscripts

Keywords

Malaria; actin; atrunculin

Introduction

With many millions of new cases of malaria reported every year, the global burden of this disease remains very high. The World Health Organization (WHO) reported 214 million cases of malaria in 2015 with approximately half a million deaths.[1] Malaria disease is primarily caused by parasites from the genus *Plasmodium* with *Plasmodium falciparum* responsible for the vast majority of deaths. This single celled eukaryotic parasite is transmitted by female *Anopheles* mosquitoes during an infectious blood feed.[2–5] Although a number of drugs are available that can effectively treat malaria, the growing resistance of the parasites to these existing treatment regimes is a major issue for future efforts to achieve sustained control or reduction of the disease globally.[6] The development of resistance implies that the current drug targets are increasingly being compromised and hence there is an urgent need to explore novel chemotherapeutic targets.

Actin is one of the most abundant proteins found in all eukaryotic cells, and is responsible for a large number of cellular functions such as cell movement, chromosomal condensation, cytoplasmic streaming, cytokinesis and maintenance of the cytoskeletal structure.[7–9] Actin can reversibly polymerise between its monomeric (G-actin) and filamentous (F-actin) form.[10, 11] Importantly, actin dynamics is an essential element involved in the cell motility and host cell invasion of malarial parasites.[11, 12] Malaria disease occurs during the blood-stage of infection, when the merozoite form of parasites invade red blood cells and replicate inside them, and actin is crucial in this invasion process. As such, any disruption in the actin dynamics could result in arrest of parasite movement, preventing it from causing disease.

A large number of natural products are known to bind to actins and thereby alter their ability to polymerize or block their ATPase activity; these compounds are therefore cytotoxic.[10] Such molecules have a specific target site on the actin molecule, often disrupting the ability of G-actin to form filaments, destabilizing the growing filament or stabilising the filament and subsequently preventing disassembly.[10] Structural analysis of the interaction between actin and bound cytotoxins reveals that several cytotoxin binding sites defined in mammalian actin are located in areas where there is marked sequence difference between human and *P. falciparum* actin.[10] Thus, compounds that selectively target such sites, with a preference for residues characterising the *P. falciparum* actin over human actin, could be used to selectively target parasite actin-dependent processes, arresting cell motility and invasion and, as such, present a potentially potent therapeutic approach to stopping malaria disease.

Latrunculins (Figure 1) are macrolides initially isolated from the marine sponge *Negombata magnifica* found in the red sea[10, 13] and are known to bind to the G-actin monomer in a 1:1 complex blocking the ability of actin to polymerize into the growing filament.[14]

The latrunculins specifically bind near the ATP binding cleft between subdomains D2 and D4 of the actin monomer[10] and thereby sequester actin away from the free cytosolic pool in

a fashion similar to that of monomer sequestering proteins.[15] We set out to identify the key differences in the latrunculin- bound binding pocket of the human and the *P. falciparum* actin in order to design a parasite-specific latrunculin-like compound. Here we describe the first steps in the development of the latrunculin actin binding interaction as a drug target for the treatment of malaria. Specifically, we describe the discovery of truncated latrunculin analogues based on a computer generated model, that when subjected to preliminary Structure Activity Relationship (SAR) studies provide the framework for the synthesis of a focused set of analogues with a 6-fold increase in their general activity and a 16-fold increase in selectivity against *P. falciparum* parasites. Critically, we can provide a structural explanation for the SAR and selectivity of these truncated analogues based on computational modelling using the parasite and human actin model structures.

Results and Discussion

Models of latrunculin-bound *P. falciparum* (*Pf*) and human (*hs*) actin were created using the 'MODELLER' program[16] with the crystal structure of rabbit muscle actin with latrunculin B bound (PDB ID: 2Q0U[17]) as the template. The alignment of *Pf* and *hs* actin sequences with that of rabbit muscle was guided by predictions of the secondary structure using the PSIPRED[18] program, and by automated sequence alignment using ClustalW; the three sequences share 79% identity and 92% similarity (Supplementary Information Figure S1). The model of *Pf* actin is almost identical to the recently solved X-ray crystal structure of this protein without ligand bound (PDB ID: 4CBU[18]); the root mean square deviation from the superimposition of Cα atoms is 0.9 Å, the most significant difference being displacement of helix α1 required to expose the ligand binding cleft.

Comparison of the binding sites of the human and the *P. falciparum* actin and identification of the key pharmacophores

Comparison of the homology models of the human and *P. falciparum* actins revealed that latrunculin B lies close to the ATP binding site and that the residues in the binding pocket are highly conserved. Only two residue differences were identified within 7 Å distance of latrunculin B, the first being the replacement of Arg206 in human actin with a Lys207 in *P. falciparum* actin, and a second difference where Met16 in human actin is replaced by Asn[17] in *P. falciparum* actin. While the ester carbonyl of latrunculin B cannot form any hydrogen bonds with Met16 in the human actin, it can engage in hydrogen bonding with Asn17 in the *P. falciparum* actin (Figure 2).

Other interactions observed in the *P. falciparum* actin model include hydrogen bonds between Glu208 and the hemiketal hydroxyl group, between Thr187 and the carbonyl of the thiazolidinone, between Tyr70 and the oxygen atom of the tetrahydropyran (THP) ring, and between Asp158 and the nitrogen atom of the thiazolidinone ring. These interactions are conserved in the human actin as well. In both cases the macrocycle is involved in hydrophobic interactions with the hydrophobic residues Pro33 and Ile35.

From these models it is clear that the thiazolidinone and the THP moiety together engage in 4 hydrogen bonds; this suggests that even in the absence of the macrocycle, a truncated molecule could interact favourably with the actin protein. The retention of biological activity

by smaller truncated fragments of a natural product is not unprecedented, with several examples apparent in the literature.[19–21] Previous studies have identified the thiazolidinone and the THP ring as the key pharmacophores involved in mammalian actin binding, while the macrocyclic ring acts to stabilise the binding by forming hydrophobic interactions.[22] Together these insights suggest a truncated latrunculin core (Figure 1) that can be derivatised at the secondary alcohol to mimic the macrocycle could retain latrunculin-like activity; significantly, removing the two *Z*-isomer double bonds of the macrocycle reduces synthetic complexity.

In consideration of the synthesis of the latrunculin core a number of important design features were addressed. The latrunculin core possesses 4 chiral centres, however, to facilitate synthetic ease the chirality about the hemiketal and the ester attached to the THP ring was not conserved. The hemiketal group, although responsible for engaging in hydrogen bonding with Glu208 (in both *P. falciparum* and human) was replaced with a methyl ketal to improve stability. The free nitrogen atom was substituted with a para-methoxybenzyl (PMB) group, since benzyl substitution had been shown to improve the activity of latrunculin A; [22] inspection of the model suggested this group could be accommodated. The latrunculin core analogue, compound **3b** (Figure 1), preserves the thiazolidinone moiety of latrunculin with its correct chirality.

Synthesis

Synthesis of the truncated latrunculin core analogue **3b**, could potentially be achieved based on the synthesis of latrunculins by Fürstner *et al.*[23, 24] or Smith *et al.*[25] Here we describe the successful synthesis of the latrunculin core analogues based on Smith *et al.*'s total synthesis of (+)-18-*epi*-latrunculol A involving alkene metathesis as the key step and utilizing Hoveyda-Grubbs' II catalyst[26–28] (Figure 3). 3-Buten-1-ol was TBS protected[29] to obtain **5** and compound **7** was prepared according to literature in 5 steps.[25] Compounds **5** and **7** were then subjected to alkene metathesis and then treated with 6 M aqueous HCl to effect Michael addition of water to the α,β-unsaturated ketone, TBS deprotection and spontaneous ring closure to obtain **9**. The hemiketal **9** was then treated with catalytic camphor sulfonic acid in methanol to obtain the methyl ketal **3b** (the latrunculin core), which was esterified using EDCI coupling to generate a focus set of analogues (Figure 4). It was found that similar to literature precedence,[23] the orientation of the secondary alcohol in the methyl ketal **3b** is largely conserved thereby resulting in the isolation of two diastereomers of **3b** (in 1:1 ratio) instead of four.

P. falciparum blood-stage growth inhibition assay and identification of truncated latrunculin analogues with low micromolar activity

The potency of the core analogues against *P. falciparum* parasites was determined by monitoring their effect on the parasite life cycle using a growth inhibition assay.[30, 31] Latrunculin B was found to be twice as potent as the latrunculin core analogue **3b** (Table 1), and the introduction of a butyl chain (**10**), a cyclopentane derivative (**11**) or a furan ring (**12**) only led to slight improvement in the activity. The benzoate derivative **13** was the first promising analogue synthesised in this series, with an EC_{50} of 31 μM. The benzoate derivatives were explored further through substitution about the phenyl ring.

The *ortho* iodo compound **14** was twice more potent than the *meta* and *para* iodo compounds **19** and **21** (respectively) and thus the *ortho* position was further explored. The higher potency of the *ortho* substituents was expected since it could mimic the presence of *Z* double bond in the natural product. This led to the synthesis of analogues **15 - 17** with 6-fold increase in activity (7 μM). It was observed that the presence of a linear chain off the *ortho* position **18** was less favoured than any of the closed ring systems.

With the *meta* substituted benzoate analogues, there was observed a two-fold increase in activity when the *meta* position had a thiophene ring (**20**) rather than an iodine atom (**19**). Similar observations were also made at the *para* position implying that a bulkier hydrophobic group was more favoured at these positions.

The activity was not greatly affected when methyl groups were incorporated at the *ortho* position of the substituted benzoate analogues (**23-25**); this meant that although further substitution using small groups along the phenyl ring were tolerated in these compounds, it did not improve the potency.

Invasion inhibition assay on *Toxoplasma gondii* (*T.gondii*) parasites

In the absence of an assay to directly determine if the latrunculin core analogues were inhibitory by specifically targeting *P. falciparum* actin in cultured blood-stage parasites, we decided to test the compounds against another parasite that shares a similar actin-binding site. *T.gondii* is the causative agent for toxoplasmosis, a widespread parasitic disease primarily affecting animals but which can also cause zoonotic infections in humans.[32] Like *P. falciparum, T. gondii* parasites are members of the Phylum Apicomplexa and share many of the conserved features of actomyosin-dependent motility. As such, they are an attractive model for studying conserved features, such as actin-dependent motility and host-cell invasion.[33, 34] Analysis of the structure of the ATP binding pocket of *T.gondii* and *P. falciparum* actins show they are identical (Supplementary Information, Figure S2). A selection of the latrunculin core analogues were then assayed in an inhibition of invasion assay to determine the potency of these analogues toward blocking invasion of *T. gondii* parasites into host fibroblast cells (Table 2).

As can be seen from Table 2, the latrunculin core analogues follow the same trend in activity with the *T. gondii* as they did with the *P. falciparum*. The ester analogues with alkyl chain (**10**) and cyclopentane ring (**11**) were inactive while the benzoate ester analogues with *ortho* substitutions (**15-17**) were active. The fact that the activity in the *P. falciparum* is mimicked by the *T. gondii* parasites supports the notion that these truncated latrunculin analogues likely target the apicomplexan actin as their binding site.

Determination of selectivity profile for the truncated latrunculin analogues

In order to determine the selectivity profile of these analogues, pyrene fluorescence and cytotoxicity assays were carried out using mammalian actin. Pyrene fluorescence is a powerful approach used to study actin filament formation based on the enhancement of fluorescence when the pyrene-labelled G-actin (monomers) assemble to form the pyrenylated actin filaments.[22, 35] Use of mammalian actin provides an indication of the

selectivity of the truncated analogues for *Plasmodium* parasites over mammalian actin (i.e. the degree of host-effect that might be occurring in an invasion context). Table 3 represents the results of the pyrene fluorescence using mammalian actin.[22] It was observed that none of the truncated analogues demonstrated a measurable decrease in the fluorescence (and thus polymerisation), indicating that these compounds do not inhibit actin filament formation, and would therefore be expected to have little effect on mammalian cells in culture. With the potent truncated analogues in the growth inhibition assay being inactive in the pyrene fluorescence assay, and the fact that latrunculin B shows 100% inhibition at a 10 μM concentration in the pyrene fluorescence assay (positive control), these combined data suggest that these synthetic truncated analogues demonstrate significant selectivity for the parasite over the mammalian actin.

Table 4 shows the results of cytotoxicity assay on a selection of truncated analogues. It can be seen that the CC_{50} values of all these compounds were ~100 μM indicating that none of these compounds showed any cytotoxicity with either the HEK293 or the HepG2 cell lines. These results showed that the truncated latrunculins were very selective towards the *P. falciparum* parasites over the mammalian and cancer cell lines.

SAR studies

A model of compound **15** in complex with *P. falciparum* actin (Figure 5) was used to establish an understanding of possible binding interactions and SAR about the truncated latrunculin analogues. As can be seen in Figure 5, the truncated latrunculin derivative **15** successfully forms interactions with Tyr70 and Asn17 as observed in the model of latrunculin B, however, interactions with Asp158 and Glu208 are lost due to PMB protection of the nitrogen atom and the methoxylation of the stereogenic center, respectively, as expected. Additionally, the hydrogen bond between the hydroxyl of Thr187 was also lost in this model, replaced by a water-mediated hydrogen bond with the carboxylate of the side-chain of Glu188 (not shown). The phenylthiophene group replaces the m acrocycle of latrunculin B, interacting across an extensive hydrophobic surface with Pro33 and Ile35. Compound **15** achieves additional hydrophobic interactions from a π stacking interaction between the side-chain of Tyr70 and the PMB group. Thus, while protection of the ketal oxygen and thiazolidinone nitrogen of the latrunculin core necessarily removed key interactions, these were replaced by new interactions that likely account for the increased activity of **15** over latrunculin B in *P. falciparum* parasites. Critically, the interaction with the single residue difference between *P. falciparum* and human actin, Asn17, is retained, accounting for the selectivity profile observed.

The surface slice of the *P. falciparum* actin model with **15** bound (Figure 6) illustrates how the ligand is predicted to be accommodated in the binding pocket. One edge of the phenylthiophene is exposed to solvent, permitting substitution of this group with larger moieties (eg. compounds **17**, **23**-**25**). Smaller groups at this position, such as compounds **3b**, **10**-**12** present a significantly smaller hydrophobic surface and consequently reduced binding affinity. The PMB packs against the hydrophobic surface offered by the side-chain of Tyr70; one edge of this group is solvent exposed, permitting exploration of larger functionalities at this position.

Conclusions

We have used homology modelling to elucidate the structure of latrunculin B bound to human and *P. falciparum* actin and have identified key differences near the ATP binding pocket. We report herein the steps towards the creation of actin inhibitors as developmental drugs for use with malaria, revealing simplified yet relatively potent and selective versions of the latrunculins that could be developed further into experimental antimalarials. Our SAR studies have led to the development of compounds **15**-**17**, each showing a 6-fold increase in activity against *P. falciparum* parasites and also an excellent selectivity profile against mammalian cell lines. Computational modelling of compound **15** bound to actin explains and validates the key interactions and SAR of these truncated latrunculin analogues. Developments in crystallography with heterologously expressed parasite actin to explore compound binding *in vitro*[18] or the use of CRISPR/Cas9 for targeted mutagenesis to *in vivo* binding, present possibilities for developing compounds like **15** further into realisable antimalarials of the future.

Experimental Section

1. Molecular Modelling

Homology modelling used the MODELLER program using the structure of rabbit muscle actin with latrunculin B bound as the template. His73 in the template is post-translationally modified (methylation); however, methylation of actin in *P. falciparum* is absent.[36] Surface exposed water molecules surrounding the template were removed, leaving only water molecules within the ligand binding region and those buried within the protein. ATP and an associated calcium ion were also included in the models.

The lowest energy homology models of the human and the *P. falciparum* actin were then subjected to energy minimisation using the program YASARA.37 The simulation cell was defined to extend 5 Å beyond all atoms, the cell boundaries were set to periodic and the cell filled with water. The YAMBER3 force field was used and the pressure was maintained at 1 bar. The energy-minimised models were then subjected to pKa prediction and cell neutralisation, followed by a very short molecular dynamics simulation of 200 ps. The models were then subjected to energy minimisation to obtain the final structures. Figures were created using the CHIMERA program.[38]

There are 4 possible diastereomers for **15**, with unresolved chiral centres about the hemiketal and THP ester linkage. The model of **15** bound to *P. falciparum* actin assumed the THP was in the chair conformation, with the phenylthiophene ester and thiazolidinone substituents in the equatorial position.

2. *P. falciparum* growth inhibition assay

The parasites chosen for this assay were at the mature pigmented trophozoite stage, and were adjusted to a starting parasitemia of 0.1% and 2% hematocrit. To 45 mL of infected red blood cells, 5 mL of stock compound was added and mixed to generate a final culture volume of 50 mL. Parasites were allowed to

develop through two cycles of erythrocyte invasion for 72 h at 37°C.[30] Glutaraldehyde (ProSciTech) was then added to the early trophozoite stage parasites after the second round of invasion, in order to fix them for 1 hour at room temperature (final concentration of 0.25% (v/v)). After fixation, the parasites were washed in human tonicity phosphate-buffered saline (HTPBS), stained with 106 SYBR green dye (Invitrogen) and 56105 red blood cells counted per well using a BD FACSCantoII flow-cytometer. Fluorescence Activated Cell Sorting (FACS) counts were analysed using FlowJoTM(Ver 6.4.7) software (Treestar). All growth inhibition assays were run in a 96-well plate format with each antibody tested in triplicate wells.

3. Invasion inhibition assay of *T. gondii*

Inhibition of invasion of *Toxoplasma* parasite growth was determined using the 2F clone of the type I RH strain that expresses the *E. coli* β-galactoside enzyme (β-Gal). A 10 mM stock solution was prepared by dissolving the compounds in DMSO and then diluted in medium containing 1% DMSO, which also served as a (compound free) control. The positive control used was the pyrazolo [3,4-d] pyrimidine inhibitor. The *T. gondii* parasites were then mixed with the compounds and preincubated for 20 min at room temperature before being used to challenge confluent monolayers of human foreskin fibroblasts (HFF) grown in 96-well plates containing Dulbecco's Modified Eagle Medium (DMEM) supplemented with 10% Fetal bovine serum (FBS). All compounds were subjected to three individual experiments, each performed in triplicates. Following addition of 5×10^2 parasites/well containing dilutions of compounds and/or 1% DMSO, plates were centrifuged at ~300g for 5 min and returned to culture at 37°C, 5% CO_2. Data were analysed using Prism (GraphPad) to determine EC_{50} values by plotting normalized, log transformed data (X axis), using nonlinear regression analysis as a sigmoidal dose-response curve with variable slope.

4. Pyrene Fluorescence assays

Unlabelled actin was mixed with pyrene-labelled actin to give a 5% labelled stock stored in calcium buffer G (CaBG: 2 mM Tris pH 8, 0.2 mM ATP, 0.5 mM DTT, 0.1 mM $CaCl_2$, 1 mM NaAzide). The stock was incubated for 2 min at room temperature with 10 × ME (final concentration 1 mM ethylene glycol teraacetic acid (EGTA), 0.1 mM $MgCl_2$) and 100 × AF (antifoam 204, Sigma) in order to convert to Mg^{2+} salt immediately prior to polymerization. This gave a final actin concentration of 2.5 μM. The pyrene-labelled actin monomer was incubated for a further 1 min with 5 μl of each compound dissolved in DMSO or latrunculin B (positive control) to a final concentration of 1 μM, 10 μM or 100 μM. Polymerisation was induced by addition and mixing of 10 × KMEI (final concentration 50 mM KCl, 10 mM imidazole pH 7, 1 mM $MgCl_2$, 1 mM EGTA), with the remaining volume made up with magnesium buffer G (MgBG: as CaBG but 0.1 mM $MgCl_2$ in place of $CaCl_2$). Immediately after, pyrene fluorescence (excitation 365 nm, emission 407 nm) was monitored in a spectrofluorometer

(Tecan Infinite M200 Pro) every 15 s for 90 min. Each assay was run in triplicate.

5. Cytotoxicity Assay

HEK293 (human embryonic kidney) and HepG2 (Hepatocellular carcinoma) cells were seeded as 3000 and 5000 cells per well, respectively, in a clear 384-well plate in a final volume of 20 μl in DMEM medium (GIBCO-Invitrogen #11995-073), in which 10% of FBS was added. Cells were incubated for 24 h at 37°C, 5% CO_2 to allow cells to attach to the plates. Compounds were prepared at 20 mM in 100% DMSO. The highest concentration to test the compounds was 100 μM, in order to maintain the DMSO final concentration at 0.5%. A dilution series 1:3 fold steps in serum free medium was created, and 20μl of each dilution was added to the cell culture wells, resulting in 5% FBS as final concentration. 100 μM tamoxifen served as negative control (all cells die) and in addition a serial dilution of tamoxifen, started at 100 μM, was included as a dose response control. The cells were incubated with the compounds for 24 h at 37°C, 5% CO_2. After the incubation, 10 μM resazurin (dissolved in Phosphate Buffered Saline (PBS)) was added to each well. The plates were then incubated for 3 h at 37°C, 5% CO_2. The fluorescence intensity (FI) was read using Polarstar Omega plate reader with excitation/emission 560/590. The data was analysed by Prism software. Results are presented as the average percentage of control for each set of triplicate wells using the following equation: Percentage Viability = $((FI_{TEST} - FI_{Negative})/(FI_{UNTREATED} - FI_{Negative}))*100$. The selectivity index was calculated using $SI = CC_{50}/EC_{50}$.

6. General Chemistry Experimental

Solvents were of analytical grade: ethyl acetate (EtOAc); dichloromethane (DCM); dimethyl formamide (DMF); methanol (MeOH); tetrahydrofuran (THF). Analytical TLC was performed on silica gel $60/F_{254}$ pre-coated aluminium sheets (0.25 mm, Merck). Flash column chromatography was carried out with silica gel 60, 0.63–0.20 mm (70–230 mesh, Merck). ^{1}H and ^{13}C NMR spectra were recorded at 400.13, and 100.62 MHz, respectively, on a Bruker Avance III Nanobay spectrometer with BACS 60 sample changer, using solvents from Cambridge Isotope Laboratories. Chemical shifts (δ, ppm) are reported relative to the solvent peak ($CDCl_3$: 7.26 [^{1}H] or 77.16 [^{13}C], DMSO-d_6: 2.50 [^{1}H] or 39.52 [^{13}C]). Proton resonances are annotated as: chemical shift (ppm), multiplicity (s, singlet; d, doublet; t, triplet; q, quartet; m, multiplet), coupling constant (*J*, Hz), and number of protons. The ^{1}H NMR spectra of diastereomer mixtures have been described separately for both diastereomers where distinct signals could be assigned. In cases where the peaks of both the diastereomers overlapped, they have been described as a single NMR spectrum. Analytical HPLC was acquired on an Agilent 1260 Infinity analytical HPLC coupled with a G1322A degasser, G1312B binary pump, G1367E high performance autosampler, G4212B diode array detector. Conditions: Zorbax Eclipse Plus C18 Rapid resolution column (4.6 × 100 mm) with UV detection at 254 nm and 214

nm, 30°C; sample was eluted using a gradient of 5 – 100% of solvent B in solvent A where solvent A: 0.1% aq. TFA, and solvent B: 0.1% TFA in CH_3CN (5 to 100% B [9 min], 100% B [1 min]; 0.5 ml/min). Low resolution mass spectrometry was performed on an Agilent 6100 Series Single Quad LCMS coupled with an Agilent 1200 Series HPLC, G1311A quaternary pump, G1329A thermostatted autosampler, and G1314B variable wavelength detector (214 and 254 nm). LC conditions: Phenomenex Luna C8(2) column (100 Å, 5 μm, 50 × 4.6 mm), 30°C; sample (5 μL) was eluted using a binary gradient (solvent A: 0.1% aq. HCO_2H; solvent B: 0.1% HCO_2H in CH_3CN; 5 to 100% B [10 min], 100% B [10 min]; 0.5 ml/min). MS conditions: quadrupole ion source with multimode-ESI; drying gas temperature, 300°C; vaporizer temperature, 200°C; capillary voltage, 2000 V (positive mode) or 4000 V (negative mode); scan range, 100–1000 *m/z*; step size, 0.1 s over 10 min. High resolution MS was performed on an Agilent 6224 TOF LCMS coupled to an Agilent 1290 Infinity LC. All data were acquired and reference mass corrected via a dual-spray electrospray ionisation (ESI) source. Each scan or data point on the total ion chromatogram (TIC) is an average of 13,700 transients, producing a spectrum every second. Mass spectra were created by averaging the scans across each peak and subtracting the background from first 10 s of the TIC. Acquisition was performed using the Agilent Mass Hunter Data Acquisition software ver. B.05.00 Build 5.0.5042.2 and analysis was performed using Mass Hunter Qualitative Analysis ver. B.05.00 Build 5.0.519.13. Acquisition parameters: mode, ESI; drying gas flow, 11 L/min; nebuliser pressure, 45 psi; drying gas temperature, 325°C; voltages: capillary, 4000 V; fragmentor, 160 V; skimmer, 65 V; octapole RF, 750 V; scan range, 100–1500 *m/z*; positive ion mode internal reference ions, *m/z* 121.050873 and 922.009798. LC conditions: Agilent Zorbax SB-C18 Rapid Resolution HT (2.1 × 50 mm, 1.8 μm column), 30°C; sample (5 μL) was eluted using a binary gradient (solvent A: 0.1% aq. HCO_2H; solvent B: 0.1% HCO_2H in CH_3CN; 5 to 100% B [3.5 min], 0.5 ml/min). Purity was determined either by analytical HPLC or by 1H NMR and was found to be ≥95% for all compounds.

General Procedure A: EDCI coupling

To the alcohol (1 eq.) dissolved in DCM (0.02 M), was added the carboxylic acid (2.8 eq.), DMAP (3 eq.) and EDCI.HCl (3 eq.). The solution was then stirred at room temperature till the completion of the reaction, as indicated by the TLC analysis. Saturated ammonium chloride solution was then added and the aqueous layer extracted with DCM (x 3). The combined organic layer was then dried with sodium sulfate and evaporated to dryness. Flash chromatography, eluting with 15% EtOAc/petroleum spirits yielded the product.

General procedure B: Suzuki coupling

To the corresponding halide (1 eq.) dissolved in 4:1 ratio of 1,4-dioxane and water (0.05 M), was added potassium carbonate (3 eq.). The solution was degassed to remove all the dissolved oxygen from the solution, before catalytic amount of $Pd(dppf)Cl_2$ (0.05 eq.) was added and the reaction mixture refluxed for 12 h. The reaction was allowed to cool to room temperature and then filtered through celite to remove most of the catalyst. The filtrate was

then diluted with EtOAc and washed with brine. The organic layer was dried with sodium sulfate and evaporated to dryness. Flash chromatography, eluting with 15% EtOAc/ petroleum spirits yielded the desired product.

4-(4-Hydroxy-2-methoxytetrahydro-2H-pyran-2-yl)-3-(4-methoxybenzyl)thiazolidin-2-one (3b)

4-(2,4-dihydroxytetrahydro-2H-pyran-2-yl)-3-(4-methoxybenzyl)thiazolidin-2-one **9** (1.14 g, 3.36 mmol) was dissolved in the corresponding alcohol (0.05 M) and catalytic CSA (0.1 eq.) was added. The reaction was stirred for 12 h before being quenched with sodium bicarbonate solution and extracted repeatedly with DCM. The combined organic layer was washed with brine and dried with sodium sulfate before evaporating to dryness to yield the product as clear oil as a mixture of two diastereomers; A and B in 1:1 ratio respectively (826 mg, 69%).

HPLC – rt 5.96 min > 98% purity at 254 nm; LRMS (only mass ion for the fragment obtained after elimination of water and methanol was observed) $[M-(H_2O + MeOH)]^+$ 304.1 m/z; HRMS $[M+H]^+$ 354.137 m/z, found 354.1355 m/z; ^{1}H NMR (diastereomer A) (400 MHz, $CDCl_3$) δ 7.23 – 7.22 (m, 2H), 6.91 – 6.82 (m, 2H), 5.20 (d, *J* = 15.4 Hz, 1H), δ 4.28 (d, *J* = 14.4 Hz, 1H), 4.11 – 3.99 (m, 1H), 3.97 – 3.91 (m, 1H), 3.86 – 3.81 (m, 1H), 3.79 (d, *J* = 1.7 Hz, 3H), 3.66 – 3.57 (m, 1H), 3.39 – 3.30 (m, 1H), 3.29 – 3.18 (m, 1H), 3.08 (s, 3H), 2.20 (ddd, *J* = 12.6, 4.6, 1.8 Hz, 1H), 1.98 – 1.88 (m, 1H), 1.67 – 1.66 (m, 1H), 1.54 – 1.38 (m, ^{1}H); ^{1}H NMR (diastereomer B) (400 MHz, $CDCl_3$) 7.14 – 7.12 (m, *J* = 8.5 Hz, 2H), 6.91 – 6.82 (m, 2H), 5.02 (d, *J* = 14.3 Hz, 1H), 4.20 (d, *J* = 15.5 Hz, 1H), 4.11 – 3.99 (m, 1H), 3.88 – 3.87 (m, 1H), 3.86 – 3.81 (m, 1H), 3.79 (d, *J* = 1.7 Hz, 3H), 3.57 – 3.48 (m, 1H), 3.39 – 3.30 (m, 1H), 3.29 – 3.18 (m, 1H), 3.01 (s, 3H), 2.10 (ddd, *J* = 12.8, 4.7, 1.8 Hz, 1H), 1.98 – 1.88 (m, 1H), 1.55 – 1.48 (m, 1H), 1.54 – 1.38 (m, 1H); ^{13}C NMR (101 MHz, $CDCl_3$) δ 159.2, 130.2, 129.0, 128.6, 114.3, 114.1, 103.3, 64.5, 60.5, 60.3, 59.3, 56.9, 55.4, 47.8, 47.6, 47.5, 46.8, 38.0, 37.35, 34.8, 34.5, 26.2, 25.4.

(But-3-en-1-yloxy)(*tert*-butyl)dimethylsilane (5)[39]

To 3-buten-1-ol **4** (3ml, 34.9 mmol) in DCM (90 ml), imidazole (4.8 mg, 70 mmol) and TBSCl (5.8 g, 38.3 mmol) was added and stirred for 20 h. On completion of the reaction, water was added to quench the reaction followed by extraction with DCM (x 3). The combined organic layer was washed with ice cold 1 M aq. HCl and then with water (x 3). The organic layer was then dried with sodium sulfate, filtered and evaporated to dryness to yield the product (6.48 g, 99% yield).

^{1}H NMR (400 MHz, $CDCl_3$) δ 5.82 (ddt, *J* = 17.1, 10.2, 6.9 Hz, 1H), 5.16 – 4.95 (m, 2H), 3.66 (t, *J* = 6.8 Hz, 2H), 2.27 (qt, *J* = 6.8, 1.3 Hz, 2H), 0.89 (s, 9H), 0.05 (s, 6H).

4-Acryloyl-3-(4-methoxybenzyl)thiazolidin-2-one (7)[25]

To *N*-methoxy-3-(4-methoxybenzyl)-*N*-methyl-2-oxothiazolidine-4-carboxamide **6** (641 mg, 2.06 mmol) in THF (7ml) at 0°C, 1.5 M vinylmagnesium bromide (7.5 mL, 10.3 mmol) was added drop wise and stirred overnight. After completion of the reaction, 2 M aq. HCl was added and then the aqueous layer extracted with DCM (x 3). The combined organic layer

was washed with saturated sodium bicarbonate solution, dried with sodium sulfate and evaporated to dryness. Flash chromatography, eluting with a gradient from 10% to 50% EtOAc/petroleum spirits led to the isolation of the product (436 mg, 93%).

^{1}H NMR (400 MHz, $CDCl_3$) δ 7.17 – 7.03 (m, 2H), 6.89 – 6.77 (m, 2H), 6.48 (dd, *J* = 17.4, 10.4 Hz, 1H), 6.35 (dd, *J* = 17.4, 1.3 Hz, 1H), 5.90 (dd, *J* = 10.4, 1.3 Hz, 1H), 5.06 (d, *J* = 14.7 Hz, 1H), 4.33 (dd, *J* = 9.4, 4.5 Hz, 1H), 3.82 (d, *J* = 14.8 Hz, 1H), 3.79 (s, 3H), 3.50 (dd, *J* = 11.5, 9.4 Hz, 1H), 3.13 (dd, *J* = 11.5, 4.5 Hz, 1H).

(*E*)-4-(5-((*tert*-Butyldimethylsilyl)oxy)pent-2-enoyl)-3-(4-methoxybenzyl)thiazolidin-2-one (8)

To 4-acryloyl-3-(4-methoxybenzyl)thiazolidin-2-one **7** (661 mg, 2.9 mmol) dissolved in DCE (16 mL) was added (but-3-en-1-yloxy)(*tert*-butyl)dimethylsilane **5** (1.1 g, 5.8 mmol) and catalytic Hoveyda-Grubbs' II catalyst (91 mg, 0.145 mmol). The reaction was then heated to 50°C for 12 h. Upon completion of the reaction, as indicated by TLC analysis, the reaction mixture was filtered through celite to remove the catalyst and then subjected to flash chromatography, eluting with 10% EtOAc/petroleum spirits to obtain the product (693 mg, 53%).

HPLC – rt 4.03 min > 99% purity at 254 nm; LRMS $[M+H]^+$ no mass ion was detected; HRMS $[M+H]^+$ 436.1972 m/z, found 436.1980 m/z; ^{1}H NMR (400 MHz, $CDCl_3$) δ 7.10 (d, *J* = 8.6 Hz, 2H), 7.00 (dt, *J* = 15.7, 7.0 Hz, 1H), 6.83 (d, *J* = 8.7 Hz, 2H), 6.25 (dt, *J* = 15.7, 1.4 Hz, 1H), 5.05 (d, *J* = 14.8 Hz, 1H), 4.27 (dd, *J* = 9.3, 4.6 Hz, 1H), 3.81 (d, 1H), 3.78 (s, 3H), 3.72 (t, *J* = 6.1 Hz, 2H), 3.46 (dd, *J* = 11.4, 9.4 Hz, 1H), 3.11 (dd, *J* = 11.4, 4.6 Hz, 1H), 2.48 – 2.34 (m, *J* = 6.3, 1.4 Hz, 2H), 0.87 (s, 9H), 0.04 (s, 6H); ^{13}C NMR (101 MHz, $CDCl_3$) δ 194.8, 172.1, 159.5, 148.7, 130.1, 127.5, 126.3, 114.3, 63.9, 61.2, 55.4, 47.3, 36.3, 28.0, 25.9, 18.3, -5.3.

4-(2,4-Dihydroxytetrahydro-2H-pyran-2-yl)-3-(4-methoxybenzyl)thiazolidin-2-one (9)

((*E*)-4-(5-((*tert*-butyldimethylsilyl)oxy)pent-2-enoyl)-3-(4-methoxybenzyl)thiazolidin-2-one)-4-(5-((tert-butyldimethylsilyl)oxy)pent-2-enoyl)-3-(4-methoxybenzyl)thiazolidin-2-one **8** (1.72 mg, 3.95 mmol) was dissolved in THF (0.05 M) and 1 M aq. HCl (0.35 M) and stirred for 12 h. The reaction was then quenched with sodium bicarbonate solution and the aqueous layer washed with DCM. The combined organic layer was washed with brine, dried with sodium sulfate and evaporated *in vacuo*. Flash chromatography eluting with 100% diethyl ether yielded the desired product as clear oil and was immediately used for the next step. (1.14 g, 85%).

2-Methoxy-2-((*R*)-3-(4-methoxybenzyl)-2-oxothiazolidin-4-yl)tetrahydro-2H-pyran-4-yl pentanoate (10)

Title compound was prepared from 4-(4-hydroxy-2-methoxytetrahydro-2H-pyran-2-yl)-3-(4-methoxybenzyl)thiazolidin-2-one **3b** (40 mg, 0.113 mmol) and valeric acid (37 μL, 0.34 mmol) according to the General Procedure A as a clear oil and a mixture of two diastereomers; A and B in 1:0.6 ratio respectively (40.4 mg, 82%).

HPLC – rt 8.62 min > 99% purity at 254 nm; LRMS $[M+Na]^+$ 460.2 m/z; HRMS $[M+H]^+$ 438.1945 m/z, found 438.1950 m/z; ^{1}H NMR (diastereomers A) (400 MHz, $CDCl_3$) δ 7.25 – 7.19 (m, 2H), 6.90 – 6.82 (m, 2H), 5.14 – 5.13 (m, 1H), 5.05 (d, *J* = 14.4 Hz, 1H), 4.28 (d, *J* = 14.4 Hz, 1H), 3.99 – 3.86 (m, 1H), 3.84 – 3.83 (m, 1H), 3.80 (s, 3H), 3.68 – 3.67 (m, 1H), 3.37 – 3.36 (m, 1H), 3.25 – 3.24 (m, 1H), 3.10 (s, 3H), 2.34 – 2.25 (m, 2H), 2.19 (ddd, *J* = 12.5, 4.8, 1.9 Hz, 1H), 1.98 – 1.97 (m, 1H), 1.69 – 1.46 (m, 4H), 1.35 – 1.34 (m, 2H), 0.96 – 0.88 (m, 3H); ^{1}H NMR (diastereomers B) (400 MHz, $CDCl_3$) δ 7.14 – 7.13 (m, 2H), 6.90 – 6.82 (m, 2H), 5.21 (d, *J* = 15.4 Hz, 1H), 5.14 – 5.13 (m, 1H), 4.20 (d, *J* = 15.5 Hz, 1H), 3.99 – 3.86 (m, 1H), 3.84 – 3.83 (m, 1H), 3.80 (s, 3H), 3.64 – 3.55 (m, 1H), 3.25 (m, 2H), 3.02 (s, 3H), 2.34 – 2.25 (m, 2H), 2.09 (ddd, *J* = 12.8, 4.9, 1.9 Hz, 1H), 1.98 – 1.97 (m, 1H), 1.80 (dd, *J* = 12.7, 11.3 Hz, 1H), 1.69 – 1.46 (m, 3H), 1.35 – 1.34 (m, 2H), 0.96 – 0.88 (m, 3H); ^{13}C NMR (101 MHz, $CDCl_3$) δ 173.4, 173.0, 159.2, 159.2, 130.2, 128.9, 128.6, 128.6, 114.3, 114.1, 103.2, 102.4, 67.0, 67.0, 60.1, 59.9, 59.2, 56.7, 55.4, 55.4, 47.7, 47.6, 47.5, 46.8, 34.4, 34.4, 34.3, 33.7, 31.2, 27.2, 26.2, 25.3, 22.4, 22.4, 13.9.

2-Methoxy-2-((*R*)-3-(4-methoxybenzyl)-2-oxothiazolidin-4-yl)tetrahydro-2H-pyran-4-yl cyclopentanecarboxylate (11)

Title compound was prepared from 4-(4-hydroxy-2-methoxytetrahydro-2H-pyran-2-yl)-3-(4-methoxybenzyl)thiazolidin-2-one **3b** (41 mg, 0.116 mmol) and cyclopentane carboxylic acid (38 μL, 0.35 mmol) according to the General Procedure A as a clear oil and a mixture of two diastereomers; A and B in 1:0.74 ratio respectively (20 mg, 38%).

HPLC – rt (diastereomer A) 9.268 min (55%), (diastereomer B) 9.297 min (45%), collectively > 99% purity at 254 nm; LRMS no mass ion was detected; HRMS $[M+H]^+$ 450.1945 m/z, found 450.1950 m/z; ^{1}H NMR (diastereomers A) (400 MHz, $CDCl_3$) δ 7.25 – 7.19 (m, 2H), 6.89 – 6.82 (m, 2H), 5.17 – 5.07 (m, 1H), 5.04 (d, *J* = 14.4 Hz, 1H), 4.28 (d, *J* = 14.4 Hz, 1H), 3.91 – 3.81 (m, 2H), 3.80 (s, 3H), 3.68 – 3.67 (m, 1H), 3.36 - 3.24 (m, 2H), 3.10 (s, 3H), 2.76 – 2.61 (m, 1H), 2.21 – 2.13 (m, 1H), 1.97 – 1.96 (m, 1H), 1.92 –1.44 (m, 10H); ^{1}H NMR (diastereomers B) (400 MHz, $CDCl_3$) δ 7.13 – 7.12 (m, 2H), 6.89 – 6.82 (m, 2H), 5.21 (d, *J* = 15.5 Hz, 1H), 5.17 – 5.07 (m, 1H), 4.20 (d, *J* = 15.5 Hz, 1H), 3.95 – 3.94 (m, 1H), 3.91 – 3.81 (m, 1H), 3.79 (s, 3H), 3.63 – 3.54 (m, 1H), 3.36 - 3.24 (m, 2H), 3.02 (s, 3H), 2.76 – 2.61 (m, 1H), 2.07 (ddd, *J* = 12.8, 4.8, 1.8 Hz, 1H), 1.97 – 1.96 (m, 1H), 1.92 – 1.44 (m, 10H); ^{13}C NMR (101 MHz, $CDCl_3$) δ 176.3, 176.2, 173.4, 173.1, 159.2, 159.2, 130.2, 129.0, 128.6, 128.6, 114.3, 114.1, 103.3, 102.5, 66.9, 66.9, 60.1, 60.0, 59.3, 56.8, 55.4, 47.7, 47.6, 47.5, 46.8, 44.0, 34.2, 33.6, 31.2, 30.2, 30.1, 30.1, 26.2, 26.0, 25.3.

2-Methoxy-2-((*R*)-3-(4-methoxybenzyl)-2-oxothiazolidin-4-yl)tetrahydro-2H-pyran-4-yl furan-2-carboxylate (12)

Title compound was prepared from 4-(4-hydroxy-2-methoxytetrahydro-2H-pyran-2-yl)-3-(4-methoxybenzyl)thiazolidin-2-one **3b** (40 mg, 0.113 mmol) and 2-furoic acid (38 mg, 0.34 mmol) according to the General Procedure A as a white semisolid and a mixture of two diastereomers; A and B in 1:0.65 ratio respectively (50.2 mg, 98%).

HPLC – rt 7.80 min > 95% purity at 254 nm; LRMS no mass ion was detected; HRMS $[M+H]^+$ 448.1424 m/z, found 448.1424 m/z; ^{1}H NMR (diastereomer A) (400 MHz, $CDCl_3$) δ

7.58 – 7.57 (m, 1H), 7.23 – 7.22 (m, 2H), 7.20 – 7.16 (m, 1H), 6.90 – 6.82 (m, 2H), 6.51 – 6.50 (m, 1H), 5.37 – 5.36 (m, 1H), 5.07 (d, *J* = 14.4 Hz, 1H), 4.29 (d, *J* = 14.4 Hz, 1H), 4.01 – 3.89 (m, 1H), 3.89 – 3.81 (m, 1H), 3.79 (s, 3H), 3.77 – 3.69 (m, 1H), 3.42 – 3.35 (m, 1H), 3.32 – 3.18 (m, 1H), 3.12 (s, 3H), 2.30 (ddd, *J* = 12.5, 4.8, 1.9 Hz, 1H), 2.10 – 2.09 (m, 1H), 1.80 (dd, *J* = 12.4, 11.5 Hz, 1H), 1.76 – 1.60 (m, 1H); ^{1}H NMR (diastereomer B) (400 MHz, $CDCl_3$) δ 7.58 – 7.57 (m, 1H), 7.20 – 7.16 (m, 1H), 7.17 – 7.11 (m, 2H), 6.90 – 6.82 (m, 2H), 6.51 – 6.50 (m, 1H), 5.37 – 5.36 (m, 1H), 5.21 (d, *J* = 15.5 Hz, 1H), 4.20 (d, *J* = 15.5 Hz, 1H), 4.01 – 3.89 (m, 1H), 3.89 – 3.81 (m, 1H), 3.80 (s, 3H), 3.69 – 3.58 (m, 1H), 3.32 – 3.18 (m, 2H), 3.04 (s, 3H), 2.20 (ddd, *J* = 12.7, 4.9, 1.9 Hz, 1H), 2.10 – 2.09 (m, 1H), 1.94 (dd, *J* = 12.7, 11.3 Hz, 1H), 1.76 – 1.60 (m, 1H); ^{13}C NMR (101 MHz, $CDCl_3$) δ 173.3, 159.3, 158.2, 146.6, 144.7, 130.2, 128.9, 128.6, 118.4, 118.3, 114.3, 114.1, 112.0, 103.3, 102.5, 68.1, 68.0, 60.1, 59.9, 59.2, 56.8, 55.4, 47.8, 47.7, 47.5, 46.8, 34.3, 33.7, 31.3, 26.2, 25.3.

2-Methoxy-2-(3-(4-methoxybenzyl)-2-oxothiazolidin-4-yl)tetrahydro-2H-pyran-4-yl benzoate (13)

Title compound was prepared from 4-(4-hydroxy-2-methoxytetrahydro-2H-pyran-2-yl)-3-(4-methoxybenzyl)thiazolidin-2-one **3b** (52.7 mg, 0.15 mmol) and benzoic acid (55 mg, 0.45 mmol) according to the General Procedure A as a white semisolid as a mixture of two diastereomers; A and B in 1: 0.8 ratio respectively (41 mg, 59%).

HPLC – rt 8.3 min > 99% purity at 254 nm; LRMS no mass ion was detected; HRMS $[M+H]^+$ 458.1632 m/z, found 458.1646 m/z; ^{1}H NMR (diastereomer A) (400 MHz, $CDCl_3$) δ 8.04 – 8.03 (m, 2H), 7.57 (t, *J* = 7.4 Hz, 1H), 7.45 (t, *J* = 7.7 Hz, 2H), 7.25 – 7.24 (m, 2H), 6.91 – 6.83 (m, 2H), 5.47 – 5.32 (m, 1H), 5.08 (d, *J* = 14.4 Hz, 1H), 4.32 (d, *J* = 14.4 Hz, 1H), 3.90 – 3.82 (m, 2H), 3.81 (s, 3H), 3.79 – 3.72 (m, 1H), 3.43 – 3.38 (m, 1H), 3.32 – 3.24 (m, 1H), 3.14 (s, 3H), 2.33 (ddd, *J* = 12.4, 4.7, 1.8 Hz, 1H), 2.17 – 2.08 (m, 1H), 1.87 – 1.77 (m, 1H), 1.69 – 1.61 (m, 1H); ^{1}H NMR (diastereomer B) (400 MHz, $CDCl_3$) δ 8.04 – 8.03 (m, 2H), 7.57 (t, *J* = 7.4 Hz, 1H), 7.45 (t, *J* = 7.7 Hz, 2H), 7.15 – 7.14 (m, 2H), 6.94 – 6.80 (m, 2H), 5.49 – 5.32 (m, 1H), 5.23 (d, *J* = 15.5 Hz, 1H), 4.22 (d, *J* = 15.5 Hz, 1H), 3.97 – 3.96 (m, 2H), 3.80 (s, 3H), 3.72 – 3.62 (m, 1H), 3.33 – 3.21 (m, 2H), 3.06 (s, 3H), 2.24 (ddd, *J* = 12.7, 4.8, 1.7 Hz, 1H), 2.16 – 2.07 (m, 1H), 1.96 (dd, *J* = 12.6, 11.3 Hz, 1H), 1.74 – 1.73 (m, 1H); ^{13}C NMR (101 MHz, $CDCl_3$) δ 173.3, 173.1, 166.0, 166.0, 159.3, 159.2, 133.2, 130.2, 129.8, 129.8, 128.9, 128.6, 128.6, 128.5, 114.3, 114.1, 103.3, 102.5, 68.0, 67.8, 60.1, 59.9, 59.3, 56.8, 55.4, 47.8, 47.7, 47.6, 46.8, 34.3, 33.7, 31.3, 27.0, 26.2, 25.3.

2-Methoxy-2-(3-(4-methoxybenzyl)-2-oxothiazolidin-4-yl)tetrahydro-2H-pyran-4-yl 2-iodobenzoate (14)

Title compound was prepared from 4-(4-hydroxy-2-methoxytetrahydro-2H-pyran-2-yl)-3-(4-methoxybenzyl)thiazolidin-2-one **3b** (151 mg, 0.43 mmol) and 2-iodobenzoic acid (318 mg, 1.28 mmol) according to the General Procedure A as a white semisolid and a mixture of two diastereomers; A and B in 1:0.9 ratio respectively (151 mg, 60%).

LRMS no mass ion was detected; HRMS $[M+H]^+$ 584.0598 m/z, found 584.0594 m/z; ^{1}H NMR (diastereomer A) (400 MHz, $CDCl_3$) δ 7.99 (d, *J* = 8.0 Hz, 1H), 7.79 (ddd, *J* = 7.8,

3.7, 1.7 Hz, 1H), 7.42 (td, *J* = 7.5, 0.9 Hz, 1H), 7.24 – 7.23 (m, 1H), 7.19 – 7.12 (m, 2H), 6.87 (dd, *J* = 8.8, 2.8 Hz, 2H), 5.49 – 5.38 (m, 1H), 5.05 (d, *J* = 14.3 Hz, 1H), 4.32 (d, *J* = 14.4 Hz, 1H), 4.00–3.92 (m, 1H), 3.91 – 3.82 (m, 1H), 3.81 (s, 3H), 3.79 – 3.71 (m, 1H), 3.44 – 3.37 (m, 1H), 3.28 – 3.27 (m, 1H), 3.14 (s, 3H), 2.38 (ddd, *J* = 12.4, 4.8, 1.9 Hz, 1H), 2.23 – 2.11 (m, 1H), 1.87 – 1.79 (dd, *J* = 12.3, 11.5 Hz, 1H), 1.71 – 1.64 (m, 1H). ^{1}H NMR (diastereomer B) (400 MHz, $CDCl_3$) δ 7.99 (d, *J* = 8.0 Hz, 1H), 7.79 (ddd, *J* = 7.8, 3.7, 1.7 Hz, 1H), 7.42 (td, *J* = 7.5, 0.9 Hz, 1H), 7.26 – 7.21 (m, 1H), 7.19 – 7.11 (m, 2H), 6.87 – 6.86 (m, *J* = 8.8, 2.8 Hz, 2H), 5.52 – 5.34 (m, 1H), 5.23 (d, *J* = 15.5 Hz, 1H), 4.23 (d, *J* = 15.5 Hz, 1H), 4.03 – 3.90 (m, 1H), 3.91 – 3.82 (m, 1H), 3.80 (s, 3H), 3.71 – 3.62 (m, 1H), 3.28 – 3.27 (m, 2H), 3.06 (s, 3H), 2.27 (ddd, *J* = 12.8, 5.1, 1.9 Hz, 1H), 2.17 – 2.16 (m, 1H), 1.99 (dd, *J* = 12.7, 11.3 Hz, 1H), 1.79 – 1.71 (m, 1H); > 95% purity by ^{1}H NMR; ^{13}C NMR (101 MHz, $CDCl_3$) δ 173.2, 172.9, 165.9, 165.8, 159.1, 159.1, 141.3, 141.3, 135.1, 134.9, 132.7, 132.7, 131.0, 130.9, 130.1, 130.1, 128.8, 128.5, 128.5, 128.0, 114.2, 114.0, 103.1, 102.4, 94.1, 94.0, 69.0, 68.9, 59.9, 59.8, 59.3, 56.7, 55.3, 55.3, 47.7, 47.6, 47.6, 46.7, 34.1, 33.6, 31.1, 31.0, 26.1, 25.3.

2-Methoxy-2-((*R*)-3-(4-methoxybenzyl)-2-oxothiazolidin-4-yl)tetrahydro-2H-pyran-4-yl 2-(thiophen-2-yl)benzoate (15)

Title compound was prepared from 2-methoxy-2-(3-(4-methoxybenzyl)-2-oxothiazolidin-4-yl)tetrahydro-2H-pyran-4-yl 2-iodobenzoate **14** (43.8 mg, 0.075 mmol) and thiophene-2-boronic acid (11.5 mg, 0.09 mmol) according to General Procedure B as a clear oil and a mixture of two diastereomers; A and B in 1:1 ratio respectively (28.4 mg, 70%).

HPLC – rt (diastereomer A) 9.00 min (52%), (diastereomer B) 9.06 min (48%), collectively > 99% purity at 254 nm; LRMS $[M+Na]^+$ 562.2 m/z; HRMS $[M+Na]^+$ 562.1329 m/z, found 562.1338 m/z; ^{1}H NMR (diastereomer A) (400 MHz, $CDCl_3$) δ 7.76 – 7.75 (m, 1H), 7.56 – 7.31 (m, 4H), 7.22 (m, 2H), 7.10 – 7.02 (m, 1H), 6.98 – 6.97 (m, 1H), 6.87 – 6.86 (m, 2H), 5.26 – 5.11 (m, 2H), 4.22 (d, *J* = 14.4 Hz, 1H), 3.91-3.71 (m, 2H), 3.87 – 3.78 (s, 3H), 3.68 – 3.59 (m, 1H), 3.37 – 3.15 (m, 2H), 3.08 (s, 3H), 2.07 (ddd, *J* = 12.5, 4.7, 1.7 Hz, 1H), 1.95 – 1.79 (m, 1H), 1.51 (dd, *J* = 12.7, 11.3 Hz, 1H), 1.47 – 1.28 (m, 1H); ^{1}H NMR (diastereomer B) (400 MHz, $CDCl_3$) δ 7.76 – 7.75 (m, 1H), 7.56 – 7.31 (m, 4H), 7.14 – 7.13 (m, 2H), 7.10 – 7.02 (m, 1H), 6.98 – 6.97 (m, 1H), 6.87 – 6.86 (m, 2H), 5.26 – 5.11 (m, 1H), 5.00 (d, *J* = 14.4 Hz, 1H), 4.18 (d, *J* = 15.5 Hz, 1H), 3.91-3.71 (m, 2H), 3.87 (s, 3H), 3.59 – 3.50 (m, 1H), 3.37 – 3.15 (m, 2H), 3.00 (s, 3H), 1.95 – 1.79 (m, 2H), 1.47 – 1.28 (m, 2H); ^{13}C NMR (101 MHz, $CDCl_3$) δ 173.2, 172.8, 168.2, 168.1, 159.2, 159.2, 142.2, 134.6, 134.5, 132.4, 132.2, 131.5, 131.4, 131.2, 131.2, 131.0, 130.2, 130.2, 129.8, 129.8, 129.6, 129.0, 128.6, 128.6, 128.0, 128.0, 127.9, 127.4, 127.3, 126.6, 126.6, 126.2, 126.0, 125.9, 114.3, 114.1, 103.1, 102.4, 68.2, 60.0, 59.9, 59.3, 56.6, 55.4, 55.4, 47.7, 47.6, 47.5, 46.7, 33.5, 33.1, 30. 8, 30.7, 26.1, 25.2.

2-Methoxy-2-((*R*)-3-(4-methoxybenzyl)-2-oxothiazolidin-4-yl)tetrahydro-2H-pyran-4-yl 2',3',4',5'-tetrahydro-[1,1'-biphenyl]-2-carboxylate (16)

Title compound was prepared from 2-methoxy-2-(3-(4-methoxybenzyl)-2-oxothiazolidin-4-yl)tetrahydro-2H-pyran-4-yl 2-iodobenzoate **14** (43.8 mg, 0.075 mmol) and cyclohexene-1-

boronic acid pinacol ester (19.6 μL, 0.09 mmol) according to General Procedure B as a clear oil and a mixture of two diastereomers; A and B in 1:1 ratio respectively (34.6 mg, 85%).

HPLC – rt (diastereomer A) 9.73 min (61%), (diastereomer B) 9.69 min (39%), collectively > 99% purity at 254 nm; LRMS $[M+Na]^+$ 560.3 m/z; HRMS $[M+H]^+$ 538.2258 m/z, found 538.2265 m/z; ^{1}H NMR (400 MHz, $CDCl_3$) δ 7.75 – 7.67 (m, 2H), 7.41 – 7.40 (m, 2H), 7.31 – 7.22 (m, 4H), 7.17 – 7.16 (m, 4H), 6.91 – 6.81 (m, 4H), 5.53 – 5.52 (m, 2H), 5.34 – 5.33 (m, 2H), 5.22 (d, *J* = 15.5 Hz, 1H), 5.06 (d, *J* = 14.3 Hz, 1H), 4.30 (d, *J* = 14.4 Hz, 1H), 4.22 (d, *J* = 15.5 Hz, 1H), 3.95 – 3.94 (m, 2H), 3.89 – 3.82 (m, 2H), 3.80 (s, 6H), 3.78 – 3.70 (m, 1H), 3.70 – 3.60 (m, 1H), 3.38 – 3.37 (m, 2H), 3.27 – 3.26 (m, 2H), 3.13 (s, 3H), 3.05 (s, 3H), 2.35 – 2.20 (m, 6H), 2.20 – 2.06 (m, 6H), 1.97 – 1.85 (m, 1H), 1.77 – 1.76 (m, 5H), 1.73 – 1.58 (m, 6H); ^{13}C NMR (101 MHz, $CDCl_3$) δ 173.1, 172.8, 168.2, 168.1, 159.2, 159.2, 145.6, 145.5, 139.1, 139.1, 131.4, 130.2, 130.2, 129.8, 129.5, 129.5, 128.9, 128.6, 128.6, 126.5, 126.5, 125.4, 125.4, 114.3, 114.1, 103.3, 102.5, 77.5, 67.9, 67.8, 66.0, 60.1, 60.0, 59.8, 59.2, 56.7, 55.4, 55.4, 47.8, 47.7, 47.5, 46.8, 34.3, 33.7, 31.2, 30.2, 30.2, 26.2, 25.6, 25.3, 23.2, 22.1.

2-Methoxy-2-((*R*)-3-(4-methoxybenzyl)-2-oxothiazolidin-4-yl)tetrahydro-2H-pyran-4-yl 2-(naphthalen-1-yl)benzoate (17)

Title compound was prepared from 2-methoxy-2-(3-(4-methoxybenzyl)-2-oxothiazolidin-4-yl)tetrahydro-2H-pyran-4-yl 2-iodobenzoate **14** (53.4 mg, 0.09 mmol) and 1-naphthaleinboronic acid (19 mg, 0.11 mmol) according to General Procedure B as a clear oil and a mixture of three diastereomers; A, B and C in 1: 0.7 : 0.5 ratios respectively (53.1 mg, 90%).

HPLC– rt 3.98 min, 4.12 min, and 4.17 min for the 3 diastereomers > 98% combined purity at 254 nm; LRMS $[M+Na]^+$ 606.2 m/z; HRMS $[M+Na]^+$ 606.1921 m/z, found 606.1935 m/z; ^{1}H NMR (400 MHz, $CDCl_3$) δ 8.15 – 6.80 (m, 33H), 5.14 (dd, *J* = 15.4, 5.4 Hz, 1H), 5.04 (d, *J* = 14.4 Hz, 0.7H), 4.98 (d, *J* = 14.4 Hz, 0.5H), 4.91 – 4.69 (m, 2.2H), 4.08 – 2.77 (m, 26.4H), 1.65 – 0.54 (m, 8.8H); ^{13}C NMR (101 MHz, $CDCl_3$) δ 173.4, 172.9, 172.7, 167.2, 167.1, 167.0, 159.2, 159.13, 141.6, 141.4, 141.3, 141.3, 140.2, 133.3, 133.3, 132.6, 132.5, 132.1, 132.0, 131.9, 131.8, 130.9, 130.8, 130.6, 130.5, 130.4, 130.2, 130.2, 130.1, 130.0, 129.3, 128.9, 128.9, 128.6, 128.5, 128.4, 128.3, 127.9, 127.8, 126.3, 126.1, 126.0, 125.9, 125.8, 125.7, 125.6, 125.3, 125.1, 114.7, 114.5, 114.4, 114.3, 114.2, 114.1, 114.0, 102.8, 102.7, 102.2, 102.1, 67.4, 67.4, 67.3, 59.7, 59.6, 59.2, 59.0, 56.7, 55.4, 47.6, 47.5, 47.3, 47.2, 46.7, 32.9, 32.5, 32.3, 30.4, 29.9, 29.7, 27.1, 26.1, 24.9, 24.9.

2-Methoxy-2-((*R*)-3-(4-methoxybenzyl)-2-oxothiazolidin-4-yl)tetrahydro-2H-pyran-4-yl 2-((*E*)-pent-1-en-1-yl)benzoate (18)

Title compound was prepared from 2-methoxy-2-(3-(4-methoxybenzyl)-2-oxothiazolidin-4-yl)tetrahydro-2H-pyran-4-yl 2-iodobenzoate **14** (15.1 mg, 0.026 mmol) and (*E*)-1-pentenylboronic acid pinacol ester (7 μL, 0.031 mmol) according to General Procedure B as a clear oil and a mixture of three diastereomers; A and B in 1: 0.7 ratios, respectively (7.8 mg, 57%). LRMS $[M+H]^+$ 526.2 m/z; HRMS $[M+H]^+$ 526.2258 m/z, found 526.2264 m/z; ^{1}H NMR (400 MHz, $CDCl_3$) δ 7.83 – 7.82 (m, 1.7H), 7.53 – 7.52 (m, 1.7H), 7.44 – 7.43 (m,

1.7H), 7.29 – 7.21 (m, 4.1H), 7.13 – 7.12 (m, 2.7H), 6.91 – 6.80 (m, 3.4H), 6.13 – 6.12 (m, 1.7H), 5.46 – 5.32 (m, 1.7H), 5.23 (d, *J* = 15.5 Hz, 0.7H), 5.07 (d, *J* = 14.3 Hz, 1H), 4.31 (d, *J* = 14.4 Hz, 1H), 4.23 (d, *J* = 15.5 Hz, 0.7H), 4.02 – 3.91 (m, 1.7H), 3.90 – 3.82 (m, 1.7H), 3.80 (m, 5.1H), 3.80 – 3.71 (m, 1H), 3.71 – 3.62 (m, 0.7H), 3.43 – 3.21 (m, 3.4H), 3.14 (s, 3H), 3.06 (s, 2.1H), 2.35 (ddd, *J* = 12.5, 4.7, 1.9 Hz, 1H), 2.28 – 2.19 (m, 4.1H), 2.19 – 2.07 (m, 1.7H), 1.95 (dd, *J* = 12.6, 11.3 Hz, 0.7H), 1.80 (dd, *J* = 12.3, 11.5 Hz, 1H), 1.76 – 1.63 (m, 1.7H), 1.53 – 1.52 (m, 3.4H), 0.97 – 0.96 (m, 5.1H); > 95% purity by ^{1}H NMR; ^{13}C NMR (101 MHz, $CDCl_3$) δ 167.3, 162.5, 153.5, 140.0, 134.0, 132.2, 131.9, 130.2, 128.7, 128.6, 127.4, 126.7, 121.0, 114.3, 1 14.1, 89.6, 67.9, 60.0, 59.3, 55.4, 47.8, 47.7, 47.6, 35.4, 31.4, 31.1, 26.2, 25.4, 22.6, 14.0.

2-Methoxy-2-(3-(4-methoxybenzyl)-2-oxothiazolidin-4-yl)tetrahydro-2H-pyran-4-yl 3-iodobenzoate (19)

Title compound was prepared from 4-(4-hydroxy-2-methoxytetrahydro-2H-pyran-2-yl)-3-(4-methoxybenzyl)thiazolidin-2-one **3b** (93 mg, 0.26 mmol) and 3-iodobenzoic acid (196 mg, 0.79 mmol) according to the General Procedure A as a yellow oil and a mixture of two diastereomers; A and B in 1: 0.6 ratio respectively (136 mg, 88%).

HPLC – rt 9.36min > 99% purity at 254 nm; LRMS no mass ion was detected; HRMS [M +H]$^{+}$ 584.0598 m/z, found 584.0607 m/z; ^{1}H NMR (400 MHz, $CDCl_3$) δ 8.35 – 8.34 (m, 1.6H), 8.04 – 7.95 (m, 1.6H), 7.92 – 7.85 (m, 1.6H), 7.25 – 7.11 (m, 4.8H), 6.92 – 6.80 (m, 3.2H), 5.39 – 5.38 (m, 1.6H), 5.23 (d, *J* = 15.5 Hz, 0.6H), 5.08 (d, *J* = 14.4 Hz, 1H), 4.32 (d, *J* = 14.4 Hz, 1H), 4.21 (d, *J* = 15.5 Hz, 0.6H), 4.03 – 3.83 (m, 3.2H), 3.81 – 3.81 (m, 4.8H), 3.78 – 3.71 (m, 1H), 3.70 – 3.63 (m, 0.6H), 3.43 – 3.21 (m, 3.2H), 3.14 (s, 3H), 3.06 (s, 1.8H), 2.32 (ddd, *J* = 12.5, 4.8, 1.9 Hz, 1H), 2.26 – 2.20 (m, 0.6H), 2.16 – 1.58 (m, 4.8H); ^{13}C NMR (101 MHz, $CDCl_3$) δ 173.1, 164.5, 159.3, 142.1, 138.6, 138.6, 132.2, 130.2, 130.2, 129.0, 128.9, 128.6, 114.3, 114.1, 103.4, 102.5, 93.9, 68.6, 68.4, 60.1, 59.9, 59.3, 56.8, 55.4, 47.8, 47.7, 47.6, 46.8, 34.3, 33.7, 31.2, 26.2, 25.4.

2-Methoxy-2-(3-(4-methoxybenzyl)-2-oxothiazolidin-4-yl)tetrahydro-2H-pyran-4-yl 3-(thiophen-2-yl)benzoate (20)

Title compound was prepared from 4-(4-hydroxy-2-methoxytetrahydro-2H-pyran-2-yl)-3-(4-methoxybenzyl)thiazolidin-2-one **3b** (40 mg, 0.11 mmol) and 3-(thiophen-2-yl)benzoic acid **26** (70 mg, 0.34 mmol) according to General Procedure A as a clear oil and a mixture of two diastereomers; A and B in 1:0.3 ratio respectively (20 mg, 32%).

HPLC – rt 9.41 min > 99% purity at 254 nm; LRMS no mass ion was detected ; HRMS [M +H]$^{+}$ 540.1509 m/z, found 540.1513 m/z; ^{1}H NMR (diastereomer A) (400 MHz, $CDCl_3$) δ 8.26 – 8.25 (m, 1H), 7.97 – 7.91 (m, 1H), 7.79 – 7.78 (m, 1H), 7.46 – 7.45 (m, 1H), 7.41 – 7.40 (m, 1H), 7.33 – 7.32 (m, 1H), 7.29 – 7.23 (m, 2H), 7.11 – 7.10 (m, 1H), 6.91 – 6.85 (m, 2H), 5.48 – 5.37 (m, 1H), 5.09 (d, *J* = 14.4 Hz, 1H), 4.34 (d, *J* = 14.4 Hz, 1H), 4.03 – 3.92 (m, 1H), 3.89 – 3.88 (m, 1H), 3.81 (s, 3H), 3.78 –3.74 (m, 1H), 3.34 – 3.21 (m, 2H), 3.15 (s, 3H), 2.35 (ddd, *J* = 12.4, 4.7, 1.8 Hz, 1H), 2.13 – 2.12 (m, 1H), 1.89 – 1.81 (m, 1H), 1.68 – 1.67 (m, 1H); ^{1}H NMR (diastereomer B) (400 MHz, $CDCl_3$) δ 8.26 – 8.25 (m, 1H), 7.97 – 7.91 (m, 1H), 7.79 – 7.78 (m, 1H), 7.46 – 7.45 (m, 1H), 7.41 – 7.40 (m, 1H), 7.33 – 7.32 (m,

1H), 7.16 – 7.15 (m, 2H), 7.11 – 7.10 (m, 1H), 6.91 – 6.85 (m, 2H), 5.48 – 5.37 (m, 1H), 5.24 (d, *J* = 15.5 Hz, 1H), 4.23 (d, *J* = 15.5 Hz, 1H), 4.03 – 3.92 (m, 1H), 3.89 – 3.88 (m, 1H), 3.81 (s, 3H), 3.73 – 3.65 (m, 1H), 3.44 – 3.39 (m, 1H), 3.34 – 3.21 (m, 1H), 3.07 (s, 3H), 2.26 – 2.25 (m, 1H), 2.13 – 2.12 (m, 1H), 1.98 – 1.97 (m, 1H), 1.68 – 1.67 (m, 1H); ^{13}C NMR (101 MHz, $CDCl_3$) δ 165.8, 159.3, 134.9, 131.0, 130.6, 130.2, 129.1, 129.0, 128.7, 128.6, 128.3, 127.1, 125.6, 124.1, 114.3, 114.1, 103.4, 68.2, 60.0, 59.3, 55.4, 47.8, 47.7, 47.6, 46.9, 33.7, 31.3, 25.4.

2-Methoxy-2-(3-(4-methoxybenzyl)-2-oxothiazolidin-4-yl)tetrahydro-2H-pyran-4-yl 4-iodobenzoate (21)

Title compound was prepared from 4-(4-hydroxy-2-methoxytetrahydro-2H-pyran-2-yl)-3-(4-methoxybenzyl)thiazolidin-2-one **3b** (93 mg, 0.26 mmol) and 4-iodobenzoic acid (195 mg, 0.79 mmol) according to the General Procedure A as a white semisolid and a mixture of two diastereomers; A and B in 1:0.6 ratio respectively (149 mg, 96%).

LRMS no mass ion was detected; HRMS $[M+H]^+$ 584.0598 m/z, found 584.0621 m/z; ^{1}H NMR (diastereomer A) (400 MHz, $CDCl_3$) δ 7.84 – 7.71 (m, 4H), 7.25 – 7.24 (m, 2H), 6.87 – 6.86 (m, 2H), 5.44 – 5.31 (m, 1H), 5.08 (d, *J* = 14.4 Hz, 1H), 4.31 (d, *J* = 14.4 Hz, 1H), 4.01 – 3.90 (m, 1H), 3.91 – 3.82 (m, 1H), 3.81 (s, 3H), 3.79 – 3.71 (m, 1H), 3.45 – 3.35 (m, 1H), 3.27 – 3.26 (m, 1H), 3.13 (s, 3H), 2.32 (ddd, *J* = 12.5, 4.8, 1.8 Hz, 1H), 2.12 – 2.11 (m, 1H), 1.81 (dd, *J* = 12.3, 11.6 Hz, 1H), 1.76 – 1.48 (m, 1H); ^{1}H NMR (diastereomer B) (400 MHz, $CDCl_3$) δ 7.84 – 7.71 (m, 4H), 7.15 – 7.14 (m, 2H), 6.87 – 6.86 (m, 2H), 5.44 – 5.31 (m, 1H), 5.23 (d, *J* = 15.5 Hz, 1H), 4.21 (d, *J* = 15.5 Hz, 1H), 4.01 – 3.90 (m, 1H), 3.91 – 3.82 (m, 1H), 3.80 (s, 3H), 3.70 – 3.60 (m, 1H), 3.27 – 3.26 (m, 2H), 3.06 (s, 3H), 2.23 (ddd, *J* = 12.6, 4.8, 1.7 Hz, 1H), 2.12 – 2.11 (m, 1H), 1.95 (dd, *J* = 12.6, 11.3 Hz, 1H), 1.76 – 1.48 (m, 1H); > 95% purity by ^{1}H NMR; ^{13}C NMR (101 MHz, $CDCl_3$) δ 173.3, 173.1, 165.5, 159.3, 159.2, 138.0, 137.8, 131.3, 131.2, 130.2, 129.8, 128.9, 128.6, 114.3, 114.1, 103.4, 102.5, 101.1, 68.4, 68.3, 60.1, 59.9, 59.3, 56.8, 55.4, 47.8, 47.7, 47.6, 46.8, 34.3, 33.7, 31.3, 26.2, 25.4.

2-Methoxy-2-((*R*)-3-(4-methoxybenzyl)-2-oxothiazolidin-4-yl)tetrahydro-2H-pyran-4-yl 4-(thiophen-2-yl)benzoate (22)

Title compound was prepared from 4-(4-hydroxy-2-methoxytetrahydro-2H-pyran-2-yl)-3-(4-methoxybenzyl)thiazolidin-2-one **3b** (50 mg, 0.14 mmol) and 4-(thiophen-2-yl)benzoic acid **27** (86 mg, 0.42 mmol) according to General Procedure A as a clear oil and a mixture of two diastereomers; A and B in 1:0.4 ratio respectively (73.9 mg, 95%).

HPLC – rt 9.41 min > 99% purity at 254 nm; LRMS $[M+Na]^+$ 562.0 m/z; HRMS $[M+H]^+$ 540.1509 m/z, found 540.1513 m/z; ^{1}H NMR (diastereomer A) (400 MHz, $CDCl_3$) δ 8.08 – 7.99 (m, 2H), 7.72 – 7.65 (m, 2H), 7.47 – 7.41 (m, 1H), 7.40 – 7.33 (m, 1H), 7.29 – 7.22 (m, 2H), 7.14 – 7.09 (m, 1H), 6.92 – 6.84 (m, 2H), 5.47 – 5.35 (m, 1H), 5.09 (d, *J* = 14.4 Hz, 1H), 4.33 (d, *J* = 14.4 Hz, 1H), 4.04 – 3.91 (m, 1H), 3.91 – 3.83 (m, 1H), 3.81 (s, 3H), 3.80 – 3.73 (m, 1H), 3.34 – 3.23 (m, 2H), 3.14 (s, 3H), 2.34 (ddd, *J* = 12.5, 4.8, 1.8 Hz, 1H), 2.21 – 2.08 (m, 1H), 1.83 (dd, *J* = 12.3, 11.5 Hz, 1H), 1.79 – 1.60 (m, 1H); ^{1}H NMR (diastereomer B) (400 MHz, $CDCl_3$) δ 8.08 – 7.99 (m, 2H), 7.72 – 7.65 (m, 2H), 7.47 – 7.41 (m, 1H), 7.40

– 7.33 (m, 1H), 7.19 – 7.14 (m, 1H), 7.14 – 7.09 (m, 2H), 6.92 – 6.84 (m, 2H), 5.47 – 5.35 (m, 1H), 5.24 (d, *J* = 15.5 Hz, 1H), 4.23 (d, *J* = 15.5 Hz, 1H), 4.04 – 3.91 (m, 1H), 3.91 – 3.83 (m, 1H), 3.80 (s, 3H), 3.72 – 3.64 (m, 1H), 3.46 – 3.37 (m, 2H), 3.07 (s, 3H), 2.26 (ddd, *J* = 12.8, 4.9, 1.8 Hz, 1H), 2.21 – 2.08 (m, 1H), 1.97 (dd, *J* = 12.6, 11.3 Hz, 1H), 1.79 – 1.60 (m, 1H); ^{13}C NMR (101 MHz, $CDCl_3$) δ 173.3, 173.1, 165.7, 159.3, 159.2, 143.2, 138.9, 130.5, 130.5, 130.2, 129.0, 128.9, 128.7, 128.6, 128.5, 126.5, 125.6, 124.7, 114.3, 114.1, 103.4, 102.6, 68.1, 67.9, 60.2, 60.0, 59.3, 56.8, 55.4, 47.8, 47.7, 47.6, 46.8, 34.4, 33.8, 31.4, 26.2, 25.4.

2-Methoxy-2-(3-(4-methoxybenzyl)-2-oxothiazolidin-4-yl)tetrahydro-2H-pyran-4-yl 5-methyl-[1,1'-biphenyl]-2-carboxylate (23)

Title compound was prepared from 2-methoxy-2-((*R*)-3-(4-methoxybenzyl)-2-oxothiazolidin-4-yl)tetrahydro-2H-pyran-4-yl 2-bromo-4-methylbenzoate **28** (41 mg, 0.074 mmol) and phenyl boronic acid (27.5 mg, 0.223 mmol) according to General Procedure B as a clear oil and a mixture of two diastereomers; A and B in 1:0.6 ratio respectively (38.4 mg, 94%).

HPLC – rt (diastereomer A) 9.42 min (53%), (diastereomer B) 9.47 min (44%), collectively > 97% purity at 254 nm; LRMS $[M+Na]^+$ 570.3 m/z; HRMS $[M+Na]^+$ 570.1921 m/z, found 570.1934 m/z; ^{1}H NMR (diastereomer A) (400 MHz, $CDCl_3$) δ 7.77 – 7.76 (m, 1H), 7.44 – 7.09 (m, 9H), 6.85 – 6.84 (m, 2H), 5.08 – 5.06 (m, 1H), 5.00 (d, *J* = 14.4 Hz, 1H), 4.19 (d, *J* = 12.0 Hz, 1H), 3.88 – 3.87 (m, 1H), 3.79 (s, 3H), 3.77 – 3.65 (m, 1H), 3.63 – 3.54 (m, 1H), 3.34 – 3.09 (m, 2H), 3.05 (s, 3H), 2.42 (s, 3H), 1.92 (ddd, *J* = 12.6, 4.7, 1.8 Hz, 1H), 1.84 – 1.67 (m, 1H), 1.35 –1.12 (m, 2H); ^{1}H NMR (diastereomer B) (400 MHz, $CDCl_3$) δ 7.77 – 7.76 (m, 1H), 7.44 – 7.09 (m, 9H), 6.85 – 6.84 (m, 2H), 5.21 (d, *J* = 15.5 Hz, 1H), 5.08 – 5.06 (m, 1H), 4.15 (d, *J* = 13.2 Hz, 1H), 3.88 – 3.86 (m, 1H), 3.79 (s, 3H), 3.77 – 3.65 (m, 1H), 3.54 – 3.44 (m, 1H), 3.34 – 3.09 (m, 2H), 2.96 (s, 3H), 2.42 (s, 3H), 1.84 – 1.67 (m, 2H), 1.35 –1.12 (m, 2H); ^{13}C NMR (101 MHz, $CDCl_3$) δ 173.1, 172.8, 168.1, 167.9, 159.2, 159.1, 143.1, 142.9, 142.0, 141.9, 141.9, 131.8, 131.6, 131.5, 130.4, 130.3, 130.2, 130.2, 130.1, 128.9, 128.6, 128.6, 128.5, 128.2, 128.1, 128.1, 128.1, 128.0, 128.0, 127.5, 127.4, 127.2, 114.3, 114.0, 103.0, 102.3, 67.7, 67.7, 59.9, 59.8, 59.2, 56.6, 55.4, 55.4, 47.6, 47.5, 47.4, 46.7, 33.4, 32.9, 30.7, 30.6, 26.1, 25.1, 21.6.

2-Methoxy-2-((*R*)-3-(4-methoxybenzyl)-2-oxothiazolidin-4-yl)tetrahydro-2H-pyran-4-yl 4-methyl-2-(thiophen-2-yl)benzoate (24)

Title compound was prepared from 2-methoxy-2-((*R*)-3-(4-methoxybenzyl)-2-oxothiazolidin-4-yl)tetrahydro-2H-pyran-4-yl 2-bromo-4-methylbenzoate **28** (46 mg, 0.083 mmol) and thiophene-2-boronic acid (32 mg, 0.25 mmol) according to General Procedure B as a yellow oil as a mixture of two diastereomers; A and B in 1:0.7 ratio respectively (40.7 mg, 89%).

HPLC - rt (diastereomer A) 9.33 min (56%), (diastereomer B) 9.34 min (43%) collectively > 99% purity at 254 nm; LRMS $[M+Na]^+$ 576.2 m/z; HRMS $[M+Na]^+$ 576.1485 m/z, found 576.1499 m/z; ^{1}H NMR (diastereomer A) (400 MHz, $CDCl_3$) δ 7.69 – 7.68 (m, 1H), 7.37 – 7.36 (m, 1H), 7.29 – 7.18 (m, 4H), 7.07 – 7.06 (m, 1H), 6.98 – 6.93 (m, 1H), 6.86 – 6.85 (m,

2H), 5.16 – 5.15 (m, 1H), 5.01 (d, *J* = 14.4 Hz, 1H), 4.22 (d, *J* = 14.4 Hz, 1H), 3.94 – 3.73 (m, 2H), 3.80 (s, 3H), 3.68 – 3.59 (m, 1H), 3.37 – 3.17 (m, 2H), 3.08 (s, 3H), 2.41 (s, 3H), 2.05 (dd, *J* = 11.8, 3.9 Hz, 1H), 1.85 – 1.84 (m, 1H), 1.46 – 1.24 (m, 2H); ^{1}H NMR (diastereomer B) (400 MHz, $CDCl_3$) δ 7.69 – 7.65 (m, 1H), 7.37 – 7.35 (m, 1H), 7.29 – 7.18 (m, 2H), 7.14 – 7.13 (m, 2H), 7.07 – 7.06 (m, 1H), 6.98 – 6.93 (m, 1H), 6.86 – 6.85 (m, 2H), 5.22 (d, *J* = 15.4 Hz, 1H), 5.16 – 5.14 (m, 1H), 4.18 (d, *J* = 15.5 Hz, 1H), 3.94 – 3.73 (m, 2H), 3.80 (s, 3H), 3.53 – 3.51 (m, 1H), 3.37 – 3.17 (m, 2H), 2.99 (s, 3H), 2.41 (s, 3H), 1.85 – 1.84 (m, 2H), 1.50 (dd, *J* = 12.8, 11.4 Hz, 1H), 1.46 – 1.24 (m, 1H); ^{13}C NMR (101 MHz, $CDCl_3$) δ 173.2, 172.8, 168.0, 167.8, 159.2, 159.1, 142.5, 141.8, 141.7, 134.8, 134.7, 132.3, 132.2, 130.2, 130.1, 130.0, 129.4, 129.2, 128.9, 128.7, 128.6, 128.5, 127.2, 126.4, 126.4, 125.9, 125.8, 114.3, 114.0, 103.1, 102.4, 67.9, 67.9, 60.0, 59.8, 59.2, 56.6, 55.4, 55.4, 47.7, 47.6, 47.4, 46.7, 33.5, 33.1, 30.8, 30.7, 26.1, 25.2, 21.5.

2-Methoxy-2-(3-(4-methoxybenzyl)-2-oxothiazolidin-4-yl)tetrahydro-2H-pyran-4-yl 5-methyl-2-(thiophen-2-yl)benzoate (25)

Title compound was prepared from 2-methoxy-2-((*R*)-3-(4-methoxybenzyl)-2-oxothiazolidin-4-yl)tetrahydro-2H-pyran-4-yl 2-bromo-5-methylbenzoate **29** (15.6 mg, 0.028 mmol) and thiophene-2-boronic acid (11 mg, 0.085 mmol) according to General Procedure B as a yellow oil and a mixture of two diastereomers; A and B in 1:0.6 ratio respectively (13.7 mg, 88%).

HPLC – rt (diastereomer A) 9.31 min (50.4%), (diastereomer B) 9.37 min (46.9%) collectively > 97% purity at 254 nm; LRMS $[M+Na]^+$ 576.2 m/z; HRMS $[M+Na]^+$ 576.1485 m/z, found 576.1498 m/z; ^{1}H NMR (diastereomer A) (400 MHz, $CDCl_3$) δ 7.56 – 7.54 (m, 1H), 7.37 – 7.32 (m, 2H), 7.33 – 7.27 (m, 1H), 7.21 – 7.20 (m, 2H), 7.06 – 7.01 (m, 1H), 6.95 – 6.94 (m, 1H), 6.91 – 6.81 (m, 2H), 5.22 – 5.12 (m, 1H), 5.01 (d, *J* = 14.4 Hz, 1H), 4.23 (d, *J* = 14.4 Hz, 1H), 3.87 (m, 1H), 3.80 (s, 3H), 3.78 – 3.71 (m, 1H), 3.69 – 3.59 (m, 1H), 3.36 – 3.16 (m, 2H), 3.08 (s, 3H), 2.42 (s, 3H), 2.11 – 2.02 (m, 1H), 1.92 – 1.81 (m, 1H), 1.43 – 1.35 (m, 1H), 1.47 – 1.23 (m, 1H); ^{1}H NMR (diastereomer B) (400 MHz, $CDCl_3$) δ 7.56 – 7.55 (m, 1H), 7.37 – 7.32 (m, 2H), 7.33 – 7.27 (m, 1H), 7.14 – 7.12 (m, 2H), 7.06 – 7.01 (m, 1H), 6.95 – 6.94 (m, 1H), 6.91 – 6.81 (m, 2H), 5.22 (d, *J* = 15.6 Hz, 1H), 5.22 – 5.12 (m, 1H), 4.18 (d, *J* = 15.6 Hz, 1H), 3.87 – 3.86 (m, 1H), 3.80 (s, 3H), 3.78 – 3.71 (m, 1H), 3.59 – 3.50 (m, 1H), 3.36 – 3.16 (m, 2H), 3.00 (s, 3H), 2.42 (s, 3H), 1.92 – 1.81 (m, 2H), 1.52 (dd, *J* = 12.7, 11.3 Hz, 1H), 1.47 – 1.23 (m, 1H); ^{13}C NMR (101 MHz, $CDCl_3$) δ 173.2, 172.8, 168.3, 168.1, 159.2, 159.2, 142.3, 138.2, 138.1, 132.2, 132.0, 131.9, 131.9, 131.7, 131.6, 131.5, 131.4, 130.3, 130.2, 130.1, 129.0, 128.7, 128.6, 127.3, 126.4, 126.4, 125.9, 125.7, 114.3, 114.1, 103.1, 102.4, 68.1, 60.0, 59.9, 59.3, 56.6, 55.4, 55.4, 47.7, 47.6, 47.5, 46.7, 33.6, 33.1, 30.8, 30.7, 26.1, 25.2, 21.1.

3-(Thiophen-2-yl)benzoic acid (26)

Title compound was prepared from 3-iodobenzoic acid (200 mg, 0.8 mmol) and thiophene-2-boronic acid (307 mg, 2.4 mmol) according to General Procedure I as a brown solid (162 mg, 99%).

HPLC – rt 6.37 min > 99% purity at 254 nm; LRMS $[M+H]^+$ 205.1 m/z; HRMS $[M+H]^+$ 205.0318 m/z, found 205.0316 m/z; ^{1}H NMR (400 MHz, $CDCl_3$) δ 8.37 (t, *J* = 1.6 Hz, 1H), 8.08 – 7.97 (m, 1H), 7.85 (ddd, *J* = 7.8, 1.9, 1.1 Hz, 1H), 7.50 (t, *J* = 7.8 Hz, 1H), 7.41 (dd, *J* = 3.6, 1.1 Hz, 1H), 7.34 (dd, *J* = 5.1, 1.1 Hz, 1H), 7.12 (dd, *J* = 5.1, 3.6 Hz, 1H); ^{13}C NMR (101 MHz, $CDCl_3$) δ 168.2, 135.1, 131.2, 130.0, 129.3, 129.1, 128.4, 127.6, 125.8, 125.0, 124.1.

4-(Thiophen-2-yl)benzoic acid (27)

Title compound was prepared from 4-iodobenzoic acid (100 mg, 0.4 mmol) and thiophene-2-boronic acid (153.6 mg, 1.2 mmol) according to General Procedure I as a brown solid (81 mg, 99%).

HPLC – rt 6.37 min > 99% purity at 254 nm; LRMS $[M+H]^+$ 205.1 m/z; HRMS $[M+H]^+$ 205.0318 205.0323 m/z, found m/z; ^{1}H NMR (400 MHz, $CDCl_3$) δ 8.17 – 8.05 (m, 2H), 7.76 – 7.67 (m, 2H), 7.45 (dd, *J* = 3.6, 1.1 Hz, 1H), 7.38 (dd, *J* = 5.1, 1.0 Hz, 1H), 7.13 (dd, *J* = 5.1, 3.7 Hz, 1H); ^{13}C NMR (101 MHz, $CDCl_3$) δ 184.4, 134.8, 131.4, 131.1, 128.5, 128.3, 127.8, 126.7, 126.7, 125.8, 124.9.

2-Methoxy-2-((*R*)-3-(4-methoxybenzyl)-2-oxothiazolidin-4-yl)tetrahydro-2H-pyran-4-yl 2-bromo-4-methylbenzoate (28)

Title compound was prepared from 4-(4-hydroxy-2-methoxytetrahydro-2H-pyran-2-yl)-3-(4-methoxybenzyl)thiazolidin-2-one (80 mg, 0.226 mmol) and 2-bromo-4-methylbenzoic acid (146 mg, 0.68 mmol) according to the General Procedure A as a white semisolid and a mixture of two diastereomers; A and B in 1:0.7 ratio respectively (71.6 mg, 57%).

HPLC – rt 9.06 min > 99% purity at 254 nm; LRMS no mass ion was detected; HRMS $[M+H]^+$ 550.0893 m/z, found 550.0907 m/z; ^{1}H NMR (400 MHz, $CDCl_3$) δ 7.71 (dd, *J* = 7.9, 2.8 Hz, 1.7H), 7.49 – 7.48 (m, 1.7H), 7.24 – 7.23 (m, 2H), 7.16 – 7.15 (m, 3.1H), 6.93 – 6.81 (m, 3.4H), 5.47 – 5.32 (m, 1.7H), 5.22 (d, *J* = 15.5 Hz, 0.7H), 5.04 (d, *J* = 14.4 Hz, 1H), 4.32 (d, *J* = 14.4 Hz, 1H), 4.23 (d, *J* = 15.5 Hz, 0.7H), 3.98 (dd, *J* = 7.3, 5.5 Hz, 0.7H), 3.96 – 3.90 (m, 1H), 3.90 – 3.82 (m, 1.7H), 3.82 – 3.78 (m, 5.1H), 3.78 – 3.70 (m, 1H), 3.70 – 3.61 (m, 0.7H), 3.49 – 3.25 (m, 3.4H), 3.13 (s, 3H), 3.05 (s, 2.1H), 2.37 (s, 5.1H), 2.33 – 2.32 (m, 1H), 2.24 (ddd, *J* = 12.7, 4.8, 1.8 Hz, 0.7H), 2.21 – 2.08 (m, 1.7H), 1.95 (dd, *J* = 12.6, 11.3 Hz, 0.7H), 1.79 – 1.61 (m, 2.7H); ^{13}C NMR (101 MHz, $CDCl_3$) δ 173.1, 165.5, 165.4, 159.3, 143.9, 135.1, 135.1, 131.6, 131.6, 130.2, 129.9, 129.0, 128.8, 128.7, 128.6, 128.1, 122.0, 114.3, 114.1, 103.3, 102.5, 68.7, 68.6, 60.1, 60.0, 59.4, 56.8, 55.4, 47.8, 47.7, 47.7, 46.9, 34.3, 33.7, 31.2, 26.2, 25.4, 21.2.

2-Methoxy-2-((*R*)-3-(4-methoxybenzyl)-2-oxothiazolidin-4-yl)tetrahydro-2H-pyran-4-yl 2-bromo-5-methylbenzoate (29)

Title compound was prepared from 4-(4-hydroxy-2-methoxytetrahydro-2H-pyran-2-yl)-3-(4-methoxybenzyl)thiazolidin-2-one (80 mg, 0.226 mmol) and 2-bromo-5-methylbenzoic acid (146 mg, 0.68 mmol) according to the General Procedure A as a clear oil and a mixture of two diastereomers; A and B in 1:0.6 ratio respectively (106.5 mg, 85%).

HPLC – rt 9.04 min > 99% purity at 254 nm; LRMS $[M+H]^+$ 550.10 m/z; HRMS $[M+H]^+$ 550.0893 m/z, found 550.0906 m/z; ^{1}H NMR (diastereomer A) (400 MHz, $CDCl_3$) δ 7.57 – 7.56 (m, 1H), 7.51 – 7.50 (m, 1H), 7.24 (d, *J* = 8.6 Hz, 2H), 7.17 – 7.09 (m, 1H), 6.90 – 6.83 (m, 2H), 5.47 – 5.34 (m, 1H), 5.04 (d, *J* = 14.4 Hz, 1H), 4.32 (d, *J* = 14.4 Hz, 1H), 4.01 – 3.90 (m, 1H), 3.86 – 3.85 (m, 1H), 3.80 (s, 3H), 3.78 – 3.70 (m, 1H), 3.41 – 3.37 (m, 1H), 3.33 – 3.22 (m, 1H), 3.13 (s, 3H), 2.39 – 2.30 (m, 4H), 2.21 – 2.09 (m, 1H), 1.85 – 1.77 (m, 1H), 1.77 – 1.59 (m, 1H); ^{1}H NMR (diastereomer B) (400 MHz, $CDCl_3$) δ 7.57 – 7.55 (m, 1H), 7.51 – 7.50 (m, 1H), 7.17 – 7.09 (m, 3H), 6.90 – 6.83 (m, 2H), 5.47 – 5.34 (m, 1H), 5.22 (d, *J* = 15.5 Hz, 1H), 4.23 (d, *J* = 15.5 Hz, 1H), 4.01 – 3.90 (m, 1H), 3.86 (m, 1H), 3.79 (s, 3H), 3.70 – 3.61 (m, 1H), 3.33 – 3.22 (m, 2H), 3.05 (s, 3H), 2.39 – 2.30 (m, 3H), 2.25 (ddd, *J* = 12.7, 4.8, 1.7 Hz, 1H), 2.21 – 2.09 (m, 1H), 1.96 (dd, *J* = 12.6, 11.4 Hz, 1H), 1.77 – 1.59 (m, 1H); ^{13}C NMR (101 MHz, $CDCl_3$) δ 173.3, 173.0, 165.7, 165.6, 159.2, 159.1, 137.4, 137.4, 134.1, 134.0, 133.6, 133.5, 131.7, 131.7, 130.1, 128.9, 128.5, 128.5, 118.3, 118.1, 114.2, 114.0, 103.2, 102.4, 68.8, 68.7, 60.0, 59.8, 59.3, 56.7, 55.3, 55.3, 47.7, 47.6, 47.6, 46.7, 34.1, 33.5, 31.0, 26.1, 25.3, 20.8.

Supplementary Material

Refer to Web version on PubMed Central for supplementary material.

Acknowledgments

We thank Rama Desai and Wilson Wong for experimental support and other members of the Baum laboratory for advice. JBB is supported by the Wellcome Trust through a New Investigator Award (100993/Z/13/Z). JGB was supported by a Senior Research Fellowship and Program Grant from the National Health and Medical Research Council of Australia, the Burnet Institute is supported by the Victorian State Government Operational Infrastructure Scheme, and the NHMRC Independent Research Institutes Infrastructure Support scheme. Red blood cells for culture were kindly provided by the Australian Red Cross Blood Service.

Abbreviations

ATP	adenosine triphosphate
PMB	paramethoxybenzyl
SAR	structure-activity relationship
THP	tetrahydropyran

References

1. Malaria, Fact Sheet. World Health Organization; Geneva: 2016. http://www.who.int/mediacentre/factsheets/fs094/en/ [accessed May 21, 2016]
2. Menard R. The journey of the malaria sporozoite through its hosts: two parasite proteins lead the way. Microbes Infect. 2000; 2:633–642. [PubMed: 10884614]
3. Cervantes S, Stout PE, Prudhomme J, Engel S, Bruton M, Cervantes M, Carter D, Tae-Chang Y, Hay ME, Aalbersberg W, Kubanek J, et al. High content live cell imaging for the discovery of new antimalarial marine natural products. BMC Infect Dis. 2012; 12:1–9. [PubMed: 22214291]
4. Calderon F, Wilson DM, Gamo FJ. Antimalarial drug discovery: recent progress and future directions. Prog Med Chem. 2013; 52:97–151. [PubMed: 23384667]

5. Hertweck C. Natural products as source of therapeutics against parasitic diseases. Angew Chem Int Ed. 2015; 54:1462–1464.
6. Gelb MH. Drug discovery for malaria: a very challenging and timely endeavor. Curr Opin Chem Biol. 2007; 11:440–445. [PubMed: 17761335]
7. Wesseling JG, Smits MA, Schoenmakers JGG. Extremely diverged actin proteins in *Plasmodium-falciparum*. Mol Biochem Parasitol. 1988; 30:143–153. [PubMed: 2459617]
8. Lee SH, Hayes DB, Rebowski G, Tardieux I, Dominguez R. Toxofilin from *Toxoplasma gondii* forms a ternary complex with an antiparallel actin dimer. Proc Natl Acad Sci U S A. 2007; 104:16122–16127. [PubMed: 17911258]
9. Oda T, Iwasa M, Aihara T, Maeda Y, Narita A. The nature of the globular- to fibrous-actin transition. Nature. 2009; 457:441–445. [PubMed: 19158791]
10. Allingham JS, Klenchin VA, Rayment I. Actin-targeting natural products: structures, properties and mechanisms of action. Cell Mol Life Sci. 2006; 63:2119–2134. [PubMed: 16909206]
11. Baum J, Papenfuss AT, Baum B, Speed TP, Cowman AF. Regulation of apicomplexan actin-based motility. Nat Rev Microbiol. 2006; 4:621–628. [PubMed: 16845432]
12. Kappe SHI, Buscaglia CA, Bergman LW, Coppens I, Nussenzweig V. Apicomplexan gliding motility and host cell invasion: overhauling the motor model. Trends Parasitol. 2004; 20:13–16. [PubMed: 14700584]
13. Kudrimoti S, Ahmed SA, Daga PR, Wahba AE, Khalifa SI, Doerksen RJ, Hamann MT. Semisynthetic latrunculin B analogs: studies of actin docking support a proposed mechanism for latrunculin bioactivity. Bioorg Med Chem. 2009; 17:7517–7522. [PubMed: 19800245]
14. Fuerstner A, Kirk D, Fenster MB, Aissa C, De Souza D, Nevado C, Tuttle T, Thiel W, Mueller O. Latrunculin analogues with improved biological profiles by "diverted total synthesis": preparation, evaluation, and computational analysis. Chem Eur J. 2007; 13:135–149. [PubMed: 17091521]
15. Kustermans G, Piette J, Legrand-Poels S. Actin-targeting natural compounds as tools to study the role of actin cytoskeleton in signal transduction. Biochem Pharmacol. 2008; 76:1310–1322. [PubMed: 18602087]
16. Sali A, Blundell TL. Comparative protein modelling by satisfaction of spatial restraints. J Mol Biol. 1993; 234:779–815. [PubMed: 8254673]
17. Allingham JS, Miles CO, Rayment I. A structural basis for regulation of actin polymerization by pectenotoxins. J Mol Biol. 2007; 371:959–970. [PubMed: 17599353]
18. Jones DT. Protein secondary structure prediction based on position-specific scoring matrices. J Mol Biol. 1999; 292:195–202. [PubMed: 10493868]
19. Crane EA, Gademann K. Capturing biological activity in natural product fragments by chemical synthesis. Angew Chem Int Ed Engl. 2016; 55:3882–3902. [PubMed: 26833854]
20. Towle MJ, Salvato KA, Budrow J, Wels BF, Kuznetsov G, Aalfs KK, Welsh S, Zheng W, Seletsky BM, Palme MH, Habgood GJ, et al. In vitro and in vivo anticancer activities of synthetic macrocyclic ketone analogues of halichondrin B. Cancer Res. 2001; 61:1013–1021. [PubMed: 11221827]
21. Lecomte N, Njardarson JT, Nagorny P, Yang G, Downey R, Ouerfelli O, Moore MA, Danishefsky SJ. Emergence of potent inhibitors of metastasis in lung cancer via syntheses based on migrastatin. Proc Natl Acad Sci U S A. 2011; 108:15074–15078. [PubMed: 21808037]
22. Khanfar MA, Youssef DTA, El Sayed KA. Semisynthetic latrunculin derivatives as inhibitors of metastatic breast cancer: biological evaluations, preliminary structure–activity relationship and molecular modeling studies. ChemMedChem. 2010; 5:274–285. [PubMed: 20043312]
23. Fuerstner A, De Souza D, Turet L, Fenster MDB, Parra-Rapado L, Wirtz C, Mynott R, Lehmann CW. Total syntheses of the actin-binding macrolides latrunculin A, B, C, M, S and 16-epi-latrunculin B. Chem Eur J. 2007; 13:115–134. [PubMed: 17091520]
24. Fürstner A, Kirk D, Fenster MDB, Aïssa C, De Souza D, Müller O. Diverted total synthesis: Preparation of a focused library of latrunculin analogues and evaluation of their actin-binding properties. Proc Natl Acad Sci U S A. 2005; 102:8103–8108. [PubMed: 15917332]
25. Williams BD, Smith AB. Total synthesis of (+)-18-epi-latrunculol A. Org Lett. 2013; 15:4584–4587. [PubMed: 23972216]

26. Garber SB, Kingsbury JS, Gray BL, Hoveyda AH. Efficient and recyclable monomeric and dendritic Ru-based metathesis catalysts. J Am Chem Soc. 2000; 122:8168–8179.
27. Jacques R, Pal R, Parker NA, Sear CE, Smith PW, Ribaucourt A, Hodgson DM. Recent applications in natural product synthesis of dihydrofuran and -pyran formation by ring-closing alkene metathesis. Org Biomol Chem. 2016; 14:5875–5893. [PubMed: 27108941]
28. Dornan PK, Lee D, Grubbs RH. Tandem olefin metathesis/oxidative cyclization: Synthesis of tetrahydrofuran diols from simple olefins. J Am Chem Soc. 2016; 138:6372–6375. [PubMed: 27133576]
29. Christensen BG, Foley Michael A, Georges Evangelinos Asimina T, Liu Tao, Porter James R, Ripka Amy S, Zhang Linping. Preparation of isoxazolidine derivatives for treatment of bacterial infections. 2006
30. Drew DR, Hodder AN, Wilson DW, Foley M, Mueller I, Siba PM, Dent AE, Cowman AF, Beeson JG. Defining the antigenic diversity of *Plasmodium falciparum* apical membrane antigen 1 and the requirements for a multi-allele vaccine against malaria. PLoS ONE. 2012; 7:e51023. [PubMed: 23227229]
31. Wilson DW, Crabb BS, Beeson JG. Development of fluorescent *Plasmodium falciparum* for in vitro growth inhibition assays. Malar J. 2010; 9:1–12. [PubMed: 20043863]
32. Lourido S, Zhang C, Lopez MS, Tang K, Barks J, Wang Q, Wildman SA, Shokat KM, Sibley LD. Optimizing small molecule inhibitors of calcium-dependent protein kinase 1 to prevent infection by *Toxoplasma gondii*. J Med Chem. 2013; 56:3068–3077. [PubMed: 23470217]
33. Meissner M, Breinich MS, Gilson PR, Crabb BS. Molecular genetic tools in *Toxoplasma* and *Plasmodium*: achievements and future needs. Curr Opin Microbiol. 2007; 10:349–356. [PubMed: 17826309]
34. Schuler H, Matuschewski K. *Plasmodium* motility: actin not actin' like actin. Trends Parasitol. 2006; 22:146–147. [PubMed: 16500149]
35. Harris ES, Rouiller I, Hanein D, Higgs HN. Mechanistic differences in actin bundling activity of two mammalian formins, FRL1 and mDia2. J Biol Chem. 2006; 281:14383–14392. [PubMed: 16556604]
36. Schmitz S, Grainger M, Howell S, Calder LJ, Gaeb M, Pinder JC, Holder AA, Veigel C. Malaria parasite actin filaments are very short. J Mol Biol. 2005; 349:113–125. [PubMed: 15876372]
37. Venselaar H, te Beek TA, Kuipers RK, Hekkelman ML, Vriend G. Protein structure analysis of mutations causing inheritable diseases. An e-Science approach with life scientist friendly interfaces. BMC Bioinf. 2010; 11:1–10.
38. Pettersen EF, Goddard TD, Huang CC, Couch GS, Greenblatt DM, Meng EC, Ferrin TE. UCSF Chimera--a visualization system for exploratory research and analysis. J Comput Chem. 2004; 25:1605–1612. [PubMed: 15264254]
39. Ghosh AK, Li J. An asymmetric total synthesis of brevisamide. Org Lett. 2009; 11:4164–4167. [PubMed: 19694486]

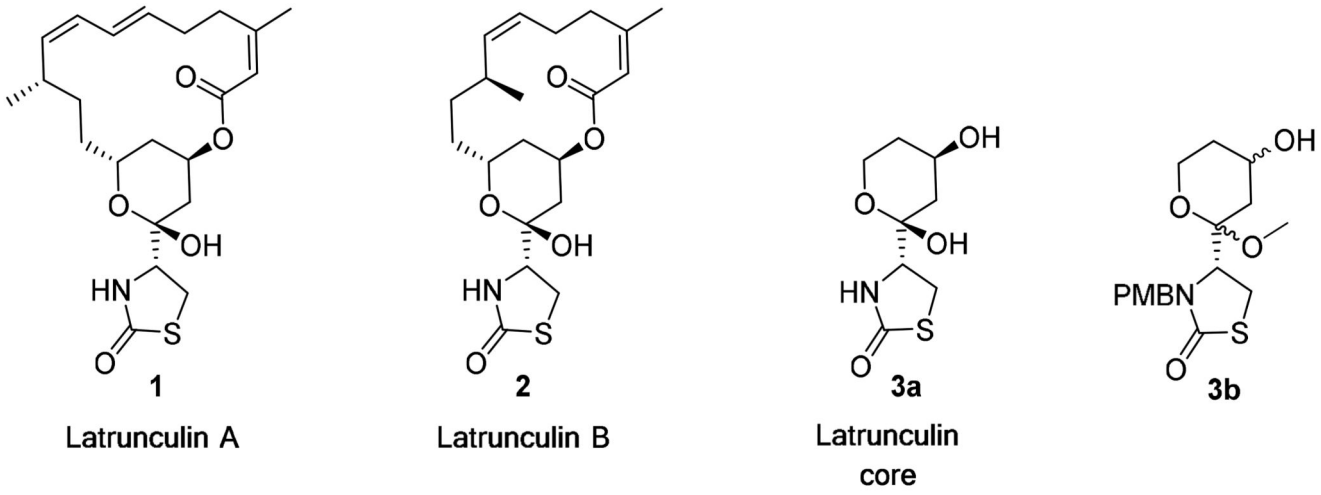

Figure 1.
Structures of latrunculin A (**1**) and B (**2**), the latrunculin core (**3a**) and the core analogue substructure (**3b**).

Europe PMC Funders Author Manuscripts

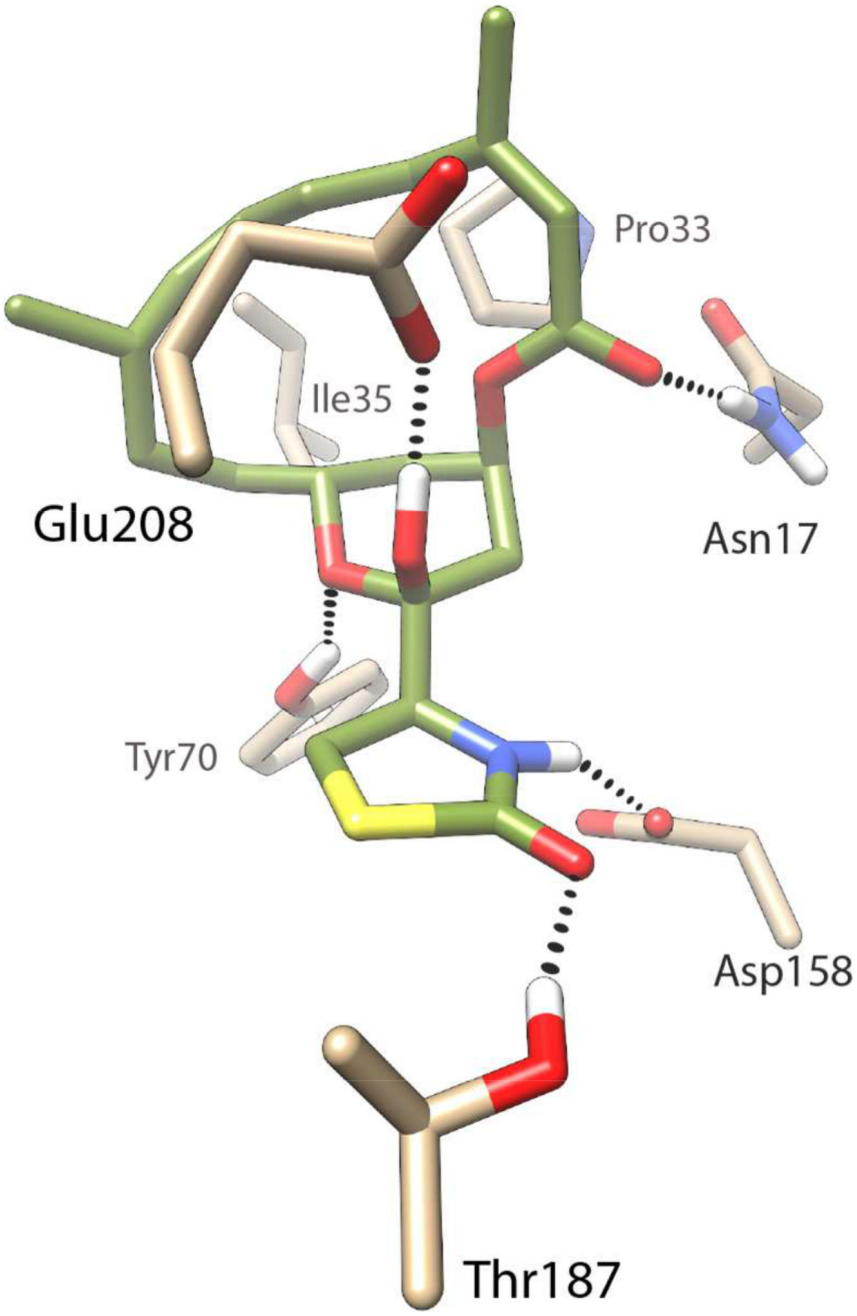

Figure 2.

Model of latrunculin B bound to *P. falciparum* actin. Latrunculin B is presented in green (and heteroatom colors), while the interacting protein residue side chains are presented in tan. Hydrogen bonds between latrunculin B and the protein are indicated by dashed lines.

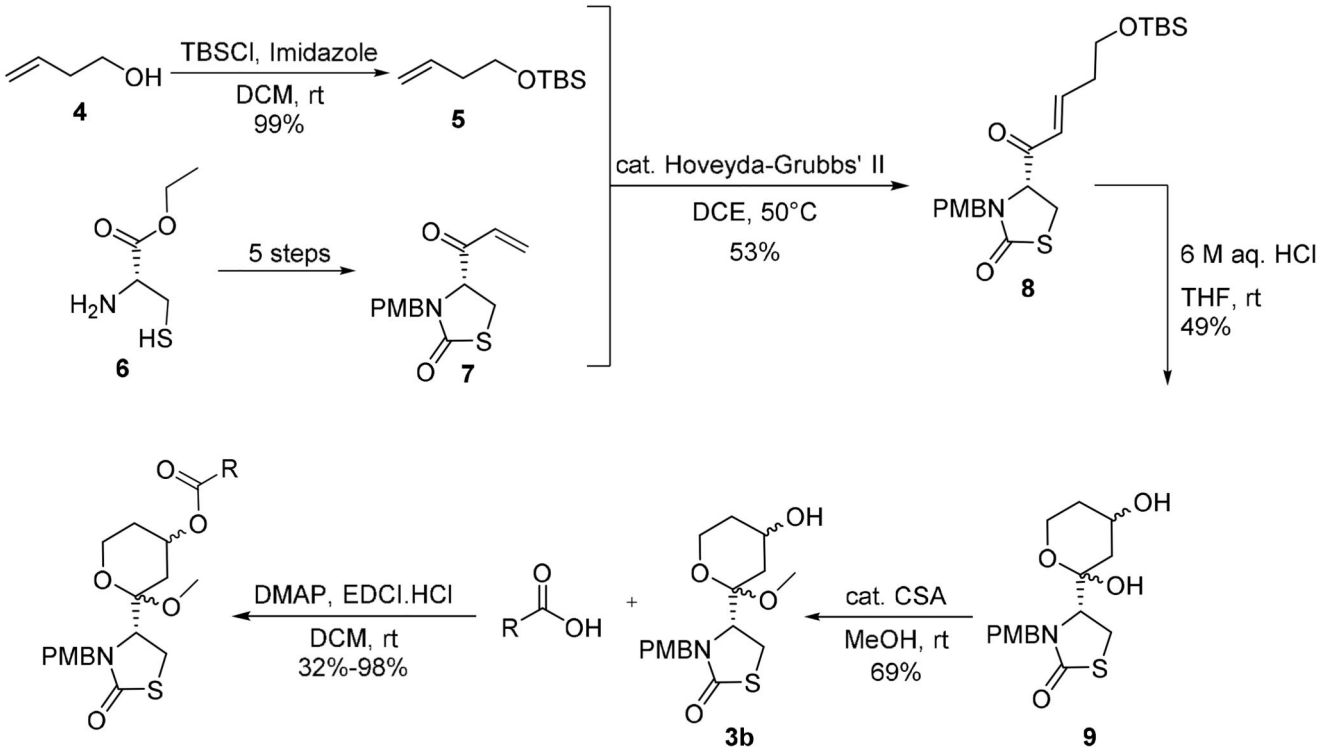

Figure 3.

Synthesis of the latrunculin core analogues based on the total synthesis of (+)-18-epi-latrunculol A.

Europe PMC Funders Author Manuscripts

Europe PMC Funders Author Manuscripts

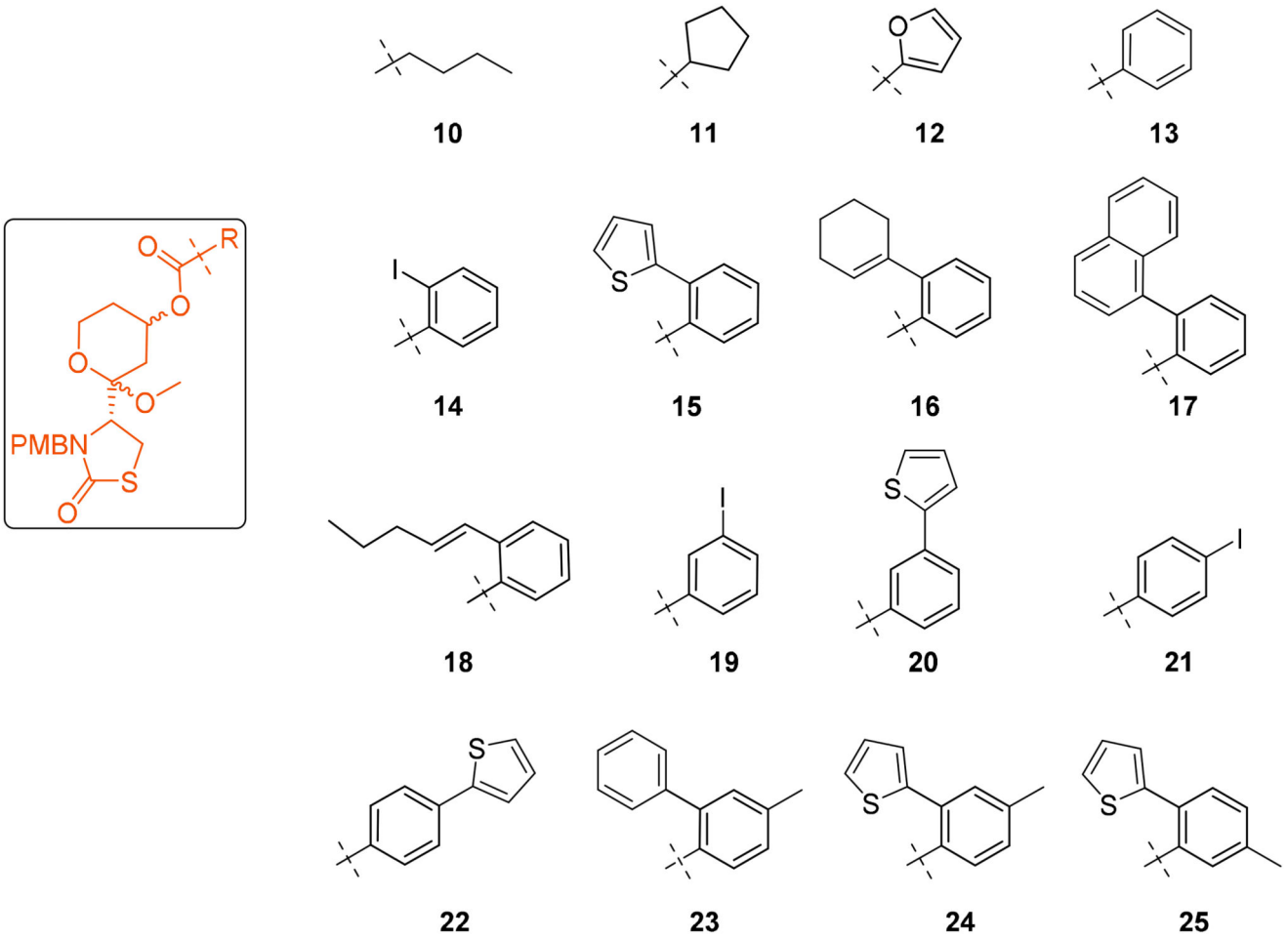

Figure 4.
The focus set of modified latrunculin core analogues.

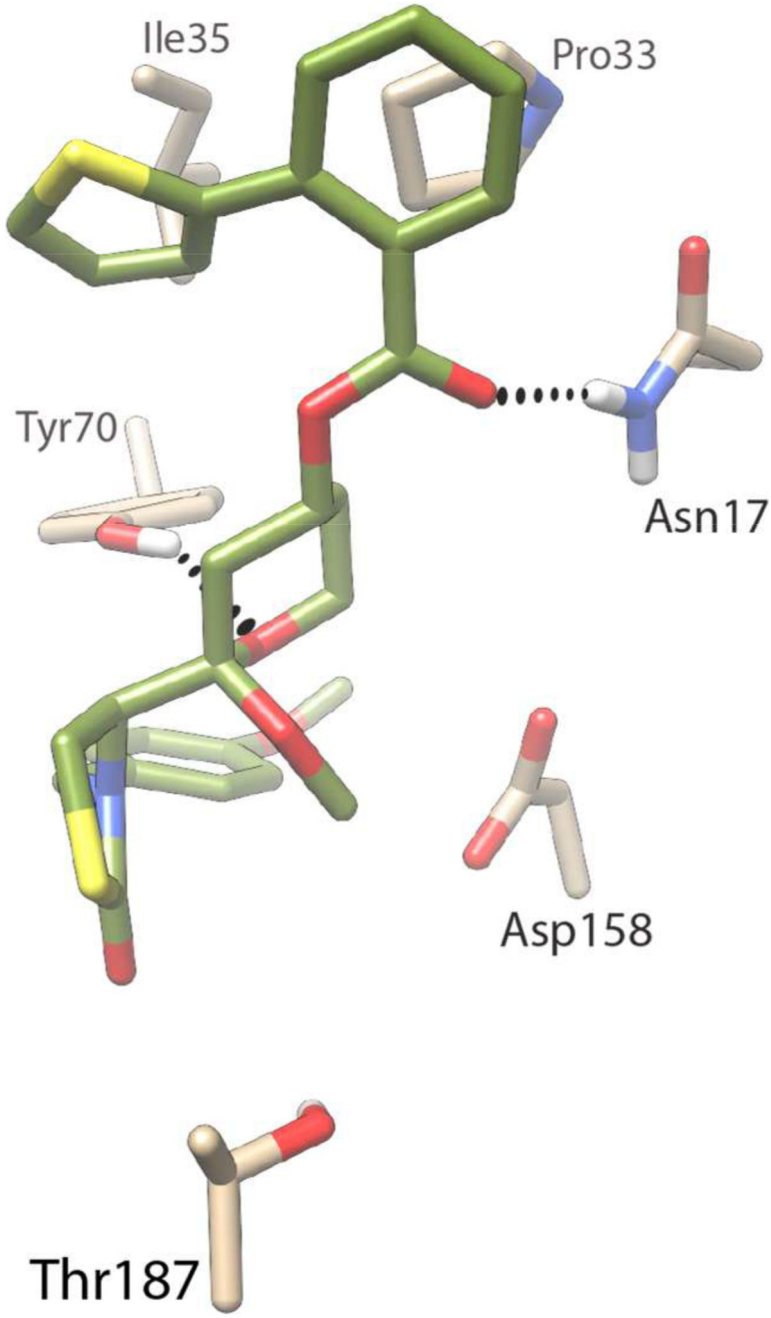

Figure 5.

Predicted binding interactions of the truncated latrunculin derivative **15** with *P. falciparum* actin. Carbon atoms of compound **15** are coloured green, and the interacting actin residues in tan; hydrogen atoms are white, nitrogen blue, and oxygen red. Hydrogen bonds between ligand and receptor are represented as dashed lines.

Europe PMC Funders Author Manuscripts

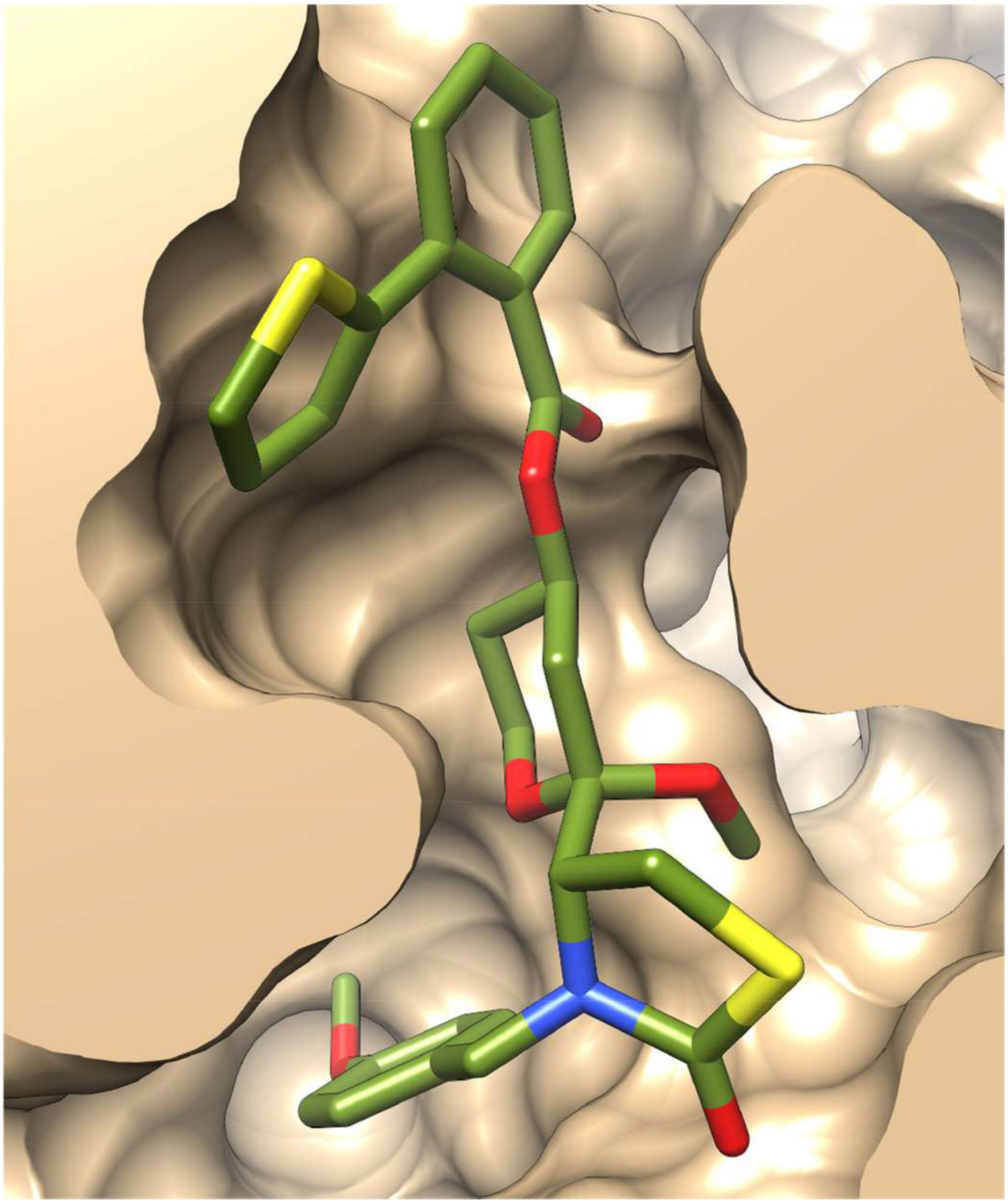

Figure 6.
Excluded volume surface of the ligand-binding site in the model of truncated latrunculin derivative **15** bound to *P. falciparum* actin.

Europe PMC Funders Author Manuscripts

Table 1

EC_{50} of actin inhibitors in *P. falciparum* blood-stage replication.

Compound	EC_{50} (μM)*	Compound	EC_{50} (μM)*
Latrunculin B	44 ± 2	**17**	7 ± 0.5
3b	>100	**18**	49 ± 3
10	66 ± 6	**19**	49 ± 1
11	66 ± 2	**20**	18 ± 3
12	62 ± 1	**21**	49 ± 3
13	31 ± 1	**22**	24 ± 12
14	17 ± 3	**23**	13 ± 1
15	7 ± 2	**24**	15 ± 3
16	7 ± 1	**25**	10 ± 2

*Data are the mean and standard deviation from a duplicate experiment.

Europe PMC Funders Author Manuscripts

Table 2

Selection of latrunculin core analogues and their corresponding activity against *T. gondii* parasites.

Compound	EC_{50} (μM)*
10	>100
11	>100
15	19 ± 1
16	16 ± 1
17	16 ± 1

* Data are the mean and standard deviation from a three individual experiments performed in triplicate.

Europe PMC Funders Author Manuscripts

Table 3

A selection of analogues with their respective percentage inhibition of mammalian actin polymerization.

Compound	Inhibition at 10 μM	Inhibition at 100 μM
Latrunculin B	100%	100%
14	<10%	<10%
15	<10%	<10%
16	<10%	<10%
17	<10%	<10%

Europe PMC Funders Author Manuscripts

Table 4

A selection of modified analogues with their respective cytotoxicity on HEK293 and HepG2 cell lines.

Compound	Cytotoxicity CC_{50} (μM)		SI	
	HEK293	HepG2	*P.falciparum* vs HEK293	*P.falciparum* vs HepG2
10	103	111	1	1
16	109	123	14	15
17	99	90	17	15